



HAL
open science

Research and development of a new combination of piezo-thermoelectric energy harvester systems from roadways.

Ando Ny Aina Randriantsoa, Damien Ali Hamada Fakra, Luc Rakotondrajaona, Riad Benelmir

► To cite this version:

Ando Ny Aina Randriantsoa, Damien Ali Hamada Fakra, Luc Rakotondrajaona, Riad Benelmir. Research and development of a new combination of piezo-thermoelectric energy harvester systems from roadways.. Engineering Research Express, 2024, 10.1088/2631-8695/ad2d98 . hal-04483273

HAL Id: hal-04483273

<https://hal.science/hal-04483273v1>

Submitted on 29 Feb 2024

HAL is a multi-disciplinary open access archive for the deposit and dissemination of scientific research documents, whether they are published or not. The documents may come from teaching and research institutions in France or abroad, or from public or private research centers.

L'archive ouverte pluridisciplinaire **HAL**, est destinée au dépôt et à la diffusion de documents scientifiques de niveau recherche, publiés ou non, émanant des établissements d'enseignement et de recherche français ou étrangers, des laboratoires publics ou privés.

Research and development of a new combination of piezo-thermoelectric energy harvester systems from roadways.

Ando Ny Aina Randriantsoa^{1,2}, Damien Ali Hamada Fakra^{3,4,*},
Luc Rakotondrajaona^{1,2}, Riad Benelmir^{3,4}

¹ Higher Institute of Technology of Antananarivo (I.S.T), Ministry of Higher Education and Scientific Research, Iadiambola Ampasampito, Po Box 8122, Antananarivo 101, Madagascar

² Engineering and Geoscience, University of Antananarivo, Antananarivo 101, Madagascar

³ University of Lorraine, Faculty of Science and Technology, Campus Aiguillettes - BP 70239 54506 Vandoeuvre-Les-Nancy, France

⁴ LERMAB Laboratory, University of Lorraine, France

E-mail: damien.fakra@univ-lorraine.fr

October 2023

Abstract. Due to the problems associated with fossil fuels, scientists and governments are investigating alternative energy sources. In recent decades, there has been an increase in interest in initiatives involving the collection of clean, limitless energy. This paper focuses on two renewable energy harvesting combination technologies: mechanical vibration utilizing piezoelectric technology and thermal sources utilizing thermoelectric technology. Existing scientific literature proposes various techniques for producing and modeling each system individually. This study proposes a novel piezo-thermoelectric pavement model with piezo-thermoelectric coupling. Due to the lack of typical experimentation in the scientific literature, a new laboratory experimental prototype proposes to reproduce artificially and simultaneously heat harvesting on the artificial road surface and mechanical vibration caused by passing vehicles. Testing the laboratory-developed prototype has determined the efficacy of the piezo-thermoelectric coupling electronic model. This study demonstrated that a hybrid piezo-thermoelectric system is more suitable for road pavement applications than a piezo-thermoelectric coupling system. A hybrid combination system can continue to produce energy even if one of the energy sources is unavailable or malfunctioning, whereas a coupling combination system cannot. In laboratory testing, the combined piezo-thermoelectric harvester proposed could generate up to $1.75 \mu W$ without optimizing the materials or power generation. This innovative study demonstrates the feasibility and applicability of combining thermoelectric and piezoelectric technology to harvest energy from road surfaces.

Keywords: energy harvesting, piezoelectric, thermoelectric, modeling, hybrid, roadway
Submitted to: *Engineering Research Express*

Highlights:

- A novel mechanical and thermal energy harvesting system for pavement is described with a piezo-thermoelectric combination
- An electronic model of the piezo-thermoelectric combination is proposed
- A low-cost laboratory prototype is designed to allow experimentation with the new piezo-thermoelectric system
- A hybrid configuration is more effective for an application of the piezo-thermoelectric system than a coupling configuration

1. Introduction

1.1. Context

Energy is currently one of the most important research topics. The form and source of energy have changed dramatically over the last century. The current challenge consists of producing enough energy to support human activities and minimizing the environmental impact of the production, utilization, and decline of energy sources. This challenge incites researchers to look for alternative energy sources apart from the current widely used fossil energy sources. These fossil energy sources are known for their pollution and depletion issues. Interest in harvesting ambient energy has increased considerably during the last few decades. Researchers have explored many harvesting technologies [1]. A brief description of these harvesting technologies is presented in the following paragraphs according to their energy sources.

1.1.1. Mechanical motion or vibration: From human movements to the vibration induced by vehicles passing on a bridge, these energy sources are available in most environments. Harvesting mechanical motion or vibration energy [2] consists of collecting this energy and converting it into electrical energy. For that purpose, piezoelectric and electromagnetic technologies are widely used. Piezoelectric transducers convert mechanical motion or vibration-induced strain into electricity. While electromagnetics exploits the relative motion inside a magnetic field to generate electricity.

1.1.2. Radio Frequency (RF): Actually, telecommunication systems make radio frequencies available in nearly all environments. Then harvesting radio frequency becomes an interest from researchers to power low-consumption devices [3]. It consists of collecting radio frequency energy through an antenna and treating that energy with a DC/DC converter and RLC circuit to convert it into exploitable electrical energy. Even if the harvested energy is still very low, interest in this research field is increasing because the remote and wireless features of radio frequency allow specific applications.

1.1.3. Temperature gradients: Thermal energy is abundant in the environment. It can be found on any device exposed to solar heat or in a running motor. Several methods allow to harvest thermal energy [4]. The use of liquid circulation to transport heat from a thermal source to heat storage. Air circulation systems work on the same principle but use air instead of liquid to transport heat. Thermoelectric materials allow for the harvest of thermal energy by directly converting temperature gradients into electricity through the Seebeck effect.

1.1.4. Solar radiation: This energy source is widely exploited, actually [5]. The main technology for harvesting solar radiation is photovoltaic panels. It consists of N-type

and P-type semiconductors where electrons are moving when the panel is exposed to solar radiation. This movement of electrons produces electrical energy. Another method allows to harvest solar radiation as solar concentration, which consists of focusing solar radiation on a specific point in order to boil a liquid and produce steam.

Some of these energy harvesting sources produce high power (for example, solar radiation for photovoltaic farms), while others produce low power (for example, piezoelectric harvesting systems), which could be used to power LEDs for lighting or self-powered devices.

In this paper, the authors examine two energy sources specific to a road system: mechanical vibration and thermal energy from the roadway [6], [7]. Energy [8] corresponds well to the principle that "nothing is lost, nothing is created, everything is transformed," attributed to Antoine De Lavoisier: Energy is not lost; it is not created but transformed. Thus, vibratory energy can be transformed into electrical energy, and the inverse transformation is also possible. In addition, thermal energy can be transformed into electrical energy.

Most studies are concerned with harnessing only one energy source, whether thermal or mechanical [9]. Energy harvesters exploiting thermal or mechanical sources have been mainly studied for self-powered small-scale devices and sensors [10], [11], [12]. The primary concern is that there will only be energy if the internal energy source is temporarily present in the system.

Combining two or more energy sources could improve the system of intermittent energy sources. In this case, even if one source of energy is unavailable, the other source can compensate.

Intermittent energy sources could be enhanced by combining two or more energy sources. In this case, even if one energy source is unavailable, the other source can compensate for the energy production [13]. This paper addresses the problems of intermittent sources by combining two energy sources (mechanical vibration and thermal gradient) in a road pavement. The main aim of this research is to develop a new experimental artificial roadway prototype for thermal and mechanical vibration harvesting. The proposed combined road energy harvesting system comprises two subsystems that generate electricity from two distinct energy sources. The suggested combination associated with the new piezo-thermoelectric coupling model described represents the originality of this work. The proposed solution introduces the possibility of coupling the two harvesting energy technologies to enhance power production from road pavement structures.

1.2. Literature review

This work aims to exploit ambient energy available on roadways. The main ambient energy sources available on roadways are the latent heat from solar radiation and mechanical energy from passing vehicles. Most works in the scientific literature generally focus on one of these energy conversion techniques. Combining mechanical vibrations

and thermal gradients is, therefore, a novel approach to study. This combination creates a hybrid harvesting device capable of addressing the issue of intermittent electricity while increasing the quantity of energy harvested [14], [15].

This section provides a summary of published articles regarding mechanical, thermal, then combined mechanical and thermal energy harvesting systems.

1.2.1. Mechanical vibration energy harvesting systems: The integration of mechanical energy harvesting systems into the infrastructure of roadways stands as a main initiative in the realm of sustainable urban development. This approach seeks to capture latent energy derived from vehicular traffic, leading toward environmentally conscious and energy-efficient urban planning. For that purpose, different technologies such as piezoelectric, electromagnetic, electrostatic, or triboelectric systems can be utilized.

Concerning piezoelectric systems, diverse approaches have been investigated in research discussions to extract energy from vibrations through this technology. Four different types of piezoelectric transducers have been studied in particular by researchers: PZT cymbal, PZT pile, PZT stack, and PZT cantilever.

Certain investigations involve the development of models for energy harvesters, with electromechanical models being widely adopted for this purpose. Khalili et al. [16] introduced a piezoelectric energy harvester designed for pavement applications. Their harvester was based on a parallel-connected stack of piezoelectric elements. An electromechanical model for this piezoelectric harvester has been proposed (see Figure 1). This electromechanical model has gained common acceptance in the literature [17]. Guo and Lu [18] have also worked on a three-degree-of-freedom electromechanical model for theoretical analysis. Their work included a feasibility validation through laboratory tests on a prototype and explored optimization strategies, resulting in a substantial increase in maximum electric power output to 300 mW under high-frequency external vibrations. A cantilevered piezoelectric energy harvester was studied by Kim et al. [19]. Their work included a model with multiple degrees of freedom, which was reduced to a single-mode model. The model is based on a thorough study of damping ratios and detailed modal analysis. The model accurately represents every part of the measured response and demonstrates that small changes in the shape of the proof mass can have a considerable effect on the efficiency of the device.

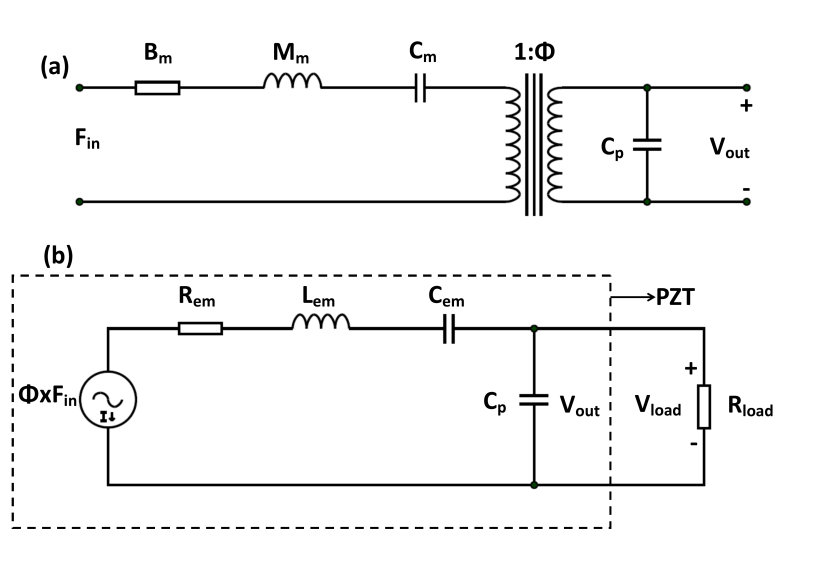


Figure 1. Mechanical model (a) and Equivalent electrical model (b) of a piezoelectric material [14]

Other investigations are concentrated on optimizing the piezoelectric element structure for enhanced energy harvesting capabilities [20, 21]. Wang et al. [22] explored the utilization of multiple layers of cantilever piezoelectric transducers, arranged in parallel under road pavements. Furthermore, the choice of ceramic material for the piezoelectric component is identified as a potential aspect to enhance the production of energy [23].

Certain research adopts a numerical methodology, as Papagiannakis et al. [24] did. Their work concerned numerical modeling to analyze stress distribution by the use of Finite Elements Method (FEM) and assess economic viability. Guo and Lu [25] explored also the utilization of FEM. The study examines laboratory-fabricated device specimens and simulates their performance in the context of actual traffic conditions. The work of Zhou et al. [26] utilized FEM on their piezoelectric harvesting system. For that purpose, they used ANSYS to simulate the behavior of the harvesting system and compared the result with theoretical and experimental data.

Vibration energy could also be harvested with electrostatic systems. Electrostatic vibration energy harvesting relies on the conversion of mechanical vibrations into electrical energy through the principle of variable capacitance. This involves the movement of charged elements in response to vibrations, leading to changes in the capacitance of the system. The variation in capacitance induces an electric potential difference, allowing for the generation of electrical power. Khan and Qadir [27] conducted a review on electrostatic energy harvesting and reported two main methods to collect vibration energy: electret-free and electret-based. In principle, the two methods remain similar. The difference is that there are electret layers added to the conductive plates of the electret-based method.

Insufficient power generation and a restricted range of operating frequencies for

electrostatic systems are the main disadvantages of this harvesting technology. Then, comprehending the fundamental threshold for energy conversion efficiency is essential for enhancing power generation. Ouro-Koura et al. [28] have evaluated the effectiveness of energy transfer compared to mixing entropy. The concept of mixing entropy, derived from statistical mechanics, is applied to describe the transfer of energy between interconnected mechanical oscillators. In their work, an analysis that does not depend on specific units compared the trends of mixing entropy with total energy. It was found that this analysis can accurately forecast the highest point of efficiency in the transfer of energy between different areas. The maximum efficacy is unaffected by the starting conditions and is determined by the square of the ratio between the nominal coupling capacitor and the natural frequency of the mechanical system.

Other approaches are also proposed in the literature to overcome these significant obstacles. The work of Li et al. [29] introduced the design of a harvester utilizing interdigitated variable capacitors and gap-closing topography. This approach utilizes electrodes with varying cross-sections and a mass without a spring. The objective is to facilitate the conversion of frequency by means of the collision of electrodes and the collision between the springless mass and the shuttle mass. Their experimentation with frequency up-conversion is confirmed by the corresponding theoretical model. Yen and Lang [30] introduced an asynchronous capacitive energy harvesting circuit that utilizes a charge pump and inductive flyback. Figure 2 demonstrates the block diagram of their harvester. The power output to a resistive load of $20M\Omega$ is $1.8\mu W$, supplied by a voltage of $6V$. The efficiency of this system is 19.1%. The harvester employs a spring steel variable capacitor, which improves the clocking process. Experimental results demonstrate a minimal starting voltage required as well as the capacity to withstand a frequency variation of up to $150Hz$. Harvesting vibration energy with an electrostatic system is mainly limited to lower power output, but the possibility of microscale application makes this technology a better option compared to other harvesting systems.

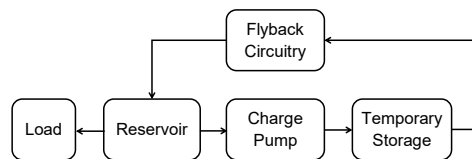


Figure 2. Block diagram of Yen and Lang’s energy harvester [30]

Electromagnetic is also a promising system to exploit vibration energy. Electromagnetic vibration harvesters consist of a magnet and a coil of wire or multiple coils arranged within a magnetic field. When the roadway experiences mechanical vibrations, such as passing vehicles, the magnet moves relative to the coil, inducing an electrical current in the wire through electromagnetic induction. As the magnet moves,

a changing magnetic flux is created through the coil of wire. According to Faraday's law of electromagnetic induction, this changing magnetic flux induces an electromotive force (EMF) or voltage across the coil. The induced voltage drives an electrical current through an external circuit connected to the coil. This technology is widely exploited in harvesting systems. The work of Li et al. [31] described the development, simulation, laboratory testing, and on-road trials of a retrofit regenerative shock absorber using a magnetic generator and rack-pinion mechanism. The shock absorber's effectiveness is enhanced by a roller steering and preload on the gear transmission, achieving a peak power of 68W.

The output power of an electromagnetic harvesting system can be improved mainly by optimizing the disposition and configuration of the system. The work of Gholikhani et al. [32] introduced a prototype for hybrid electromagnetic energy harvesting, consisting of a linear generator and a rack-pinion system. The prototype, designed as a speed bump, demonstrated potential for real-world applications. Important factors that affect power generation were found through experiments and mathematical models. For example, magnetic flux and relative movement in the linear generator mechanism and vertical velocity and gearbox ratio in the rack-pinion mechanism. Their prototype generated 1.2W for the rack pinion and 80mW for the linear generator. The recent work of Zhang et al. [33] presents a novel electromagnetic vibration energy harvester designed for self-powered freight train sensors. The harvester uses a series coupling input mechanism, reducing the moment exerted on the vibration source. The design uses two gears to convert vertical oscillations into bidirectional rotation, producing electrical energy. Their experimentation demonstrated a power of 10.219W and an efficiency of 64.31%. Supercapacitors and rectifier voltage regulator modules are used for efficient storage. Electromagnetic harvesting systems are able to produce higher output power compared to other technologies but are limited when it concerns microscale applications.

Triboelectric systems are another way to exploit vibrational energy. Triboelectric energy harvesters consist of two materials with different triboelectric properties. Typically, one material tends to gain electrons (positive triboelectric material) and another tends to lose electrons (negative triboelectric material). When these materials come into contact and then separate, a voltage is generated between the two materials due to the transfer of electrons. Several applications involve triboelectric harvesters. Lu et al. [34] proposed a sector-shaped triboelectric nanogenerator (TENG) to gather data on driver behavior, including accelerator and brake pedal activation and steering angle measurement. Their triboelectric system has a high sensitivity and can generate up to 10V of output voltage. This self-powered sensor demonstrates the practicality of TENG in intelligent transportation systems.

To increase the amount of harvested energy from the triboelectric system, the configuration of the harvesting system can be optimized. The study of Yang et al. [35] presents a triple-cantilever-based triboelectric nanogenerator designed for vibration energy. The device uses nanowire arrays in beryllium-copper alloy foils, generating up to 101V and 55.7 μ A. A peak power density of 252.3mW/m² is observed on

their prototype under a resonance frequency of $3.7Hz$. Their work assumes that the proposed triboelectric harvester could empower 40 LEDs. Ibrahim et al. [36] explored the efficiency and cost-effectiveness of triboelectric mechanisms for sustainable power generation. The triboelectric harvesting system consist of aluminum and polydimethylsiloxane layers, with an additional aluminum electrode. Their study reported that the impact amplifies the force on the layers, resulting in increased stiffness and a broader frequency bandwidth. The experimentation demonstrate an output of $05.5V$ and $15\mu W$ under $0.8g$ vibration amplitude.

These different technologies allow harvesting energy from mechanical vibration. The choice of the technology to be adopted depends on several factors, such as the frequency and amplitude of the vibration source, power requirements, environment and operating conditions, size and weight constraints, cost and manufacturing complexity, integration, and compatibility. The compatibility of the vibration harvester with the existing system or structure is important for seamless integration and optimal performance. Considerations such as mechanical and electrical interfaces, mounting options, and connectivity requirements play a role in the choice of harvester. For that purpose, table 1 summarizes the main advantages and limitations of vibration energy sources.

Vibration harvesting technology	Advantages	Limitations
Piezoelectric	<ul style="list-style-type: none"> - Easier application, simple structure [37] - Easier output voltage rectification [27] - Not easily affected by electromagnetic waves [37] - Do not need external energy source [27] - Higher power density [38] 	<ul style="list-style-type: none"> - Depolarization [37] - Lower electromagnetic coupling for PZT [37] - Higher output impedance [27] - Lower output current [27] - Need piezoelectric material [27]
Electromagnetic	<ul style="list-style-type: none"> - High energy density [37] - Do not require smart materials [37] - Lower cost [37] - Do not need mechanical friction [27] - Higher output current [27] - Lower output impedance [27] 	<ul style="list-style-type: none"> - Difficult to design in micro scale [37] - Interaction with electromagnetic waves [37] - Lower output voltage [27] - Coils contain ohmic loss [27]
Electrostatic	<ul style="list-style-type: none"> - Do not need smart material [37] - Suitable for minituarization [37] - Adapted for low frequency [27] - Higher electrical damping [27] - Higher output voltage [27] 	<ul style="list-style-type: none"> - Lower energy density [37] - May need external source [37] - High output impedance [37] - Low capacitance [27]
Triboelectric	<ul style="list-style-type: none"> - Large frequency application [39] - Lower cost [39] - Adapted for low frequency [35] - High power density [35] 	<ul style="list-style-type: none"> - Low power output [40] - Depend on triboelectric materials [40] - Fatigue of triboelectric materials [40]

Table 1. Comparison analysis of existing vibration energy harvesting system

1.2.2. Thermal energy harvesting systems: In the field of energy harvesting from roads, thermal energy is another potential energy source. The road is exposed to solar radiation during the day. The asphalt layer is heated up and keeps this thermal energy within its thickness for hours. High temperatures are not necessarily adapted for the reliability of asphalt. Consequently, researchers are looking to exploit this latent energy. In the literature, several technologies allow for the collection of this thermal energy

and the transformation of it into electric energy using pipe systems or thermoelectric generators.

The pipe system consists of This is different from common methods that use a system of a network of pipes embedded under an asphalt layer. A fluid (air or liquid) is circulating inside the pipe network. When the asphalt layer is heated up by solar radiation, this thermal energy is transmitted to the pipe system. Then the temperature difference between circulating hot and cold fluids is used for energy extraction or stored in energy reservoirs to be exploited later[41, 42, 43, 44, 45, 46].

Pipe systems are often exploited with thermoelectric generators. The hot fluid circulating in the pipe network is connected to the face of the thermoelectric generator. The other face of the thermoelectric generator is connected to another pipe network, where cold fluid is circulating. The temperature difference between the hot and cold faces of the thermoelectric generator produces a voltage that can be exploited as an electric energy source. The work of Guo and Lu [47] has estimated that a pipe system combined with a thermoelectric generator could generate about 55 GWh of energy per day if the system is deployed to the entire Florida roadway network.

However, the use of pipe systems in pavements faces significant challenges. The main concern is their vulnerability to damage under high or intense traffic loads, which can harm their structure. Additionally, the complexities of these pipe systems create logistical problems for maintenance, especially in cases of leaks [47]. These operational challenges highlight the need for alternative and robust strategies for pavement energy harvesting.

In response to these challenges, a promising approach involves directly incorporating thermoelectric modules into pavement layers. This method generates electricity from temperature differences within the layers of pavement using the Seebeck effect. This provides a more robust and feasible solution. Jiang et al. [12] have made significant progress in this area with their "Road Thermoelectric Generator System" (RTEGS). The objectives of their study are to exploit ambient thermal energy, maximize the temperature gap and consequently maximize energy production, and mitigate the urban heating island effect and structural impact of high temperatures on asphalt structures.

To achieve this objective, Jiang et al. [12] implemented vapor chambers within the pavement. These chambers serve to conduct the heat energy from the road to the Thermoelectric Generators (TEG), which are installed on the roadside. This is the hot segment of the thermoelectric system. The cold segment is connected to a water tank. Subsequently, the thermoelectric generators are arranged in series to generate electricity by harnessing the temperature differential between the hot and cold sections. This approach improves the sustainability and reliability of pavement-based energy harvesting but also introduces a resilient solution that overcomes the limitations associated with common pipe systems. The addition of thermoelectric modules directly to pavement layers shows promise for both long-lasting performance and easier maintenance. This is a big step toward using energy-harvesting technologies in real-life infrastructure situations.

Datta et al. [48] developed another way to capture energy using thermoelectrics.

Instead of a vapor chamber, their prototype used a Z-shaped copper plate with thermal isolation to transport heat from the road to the thermoelectric generator (see Figure 3). The bottom part of this thermoelectric system was connected to a heat sink filled with water to make the temperature difference as large as possible and increase the captured energy.

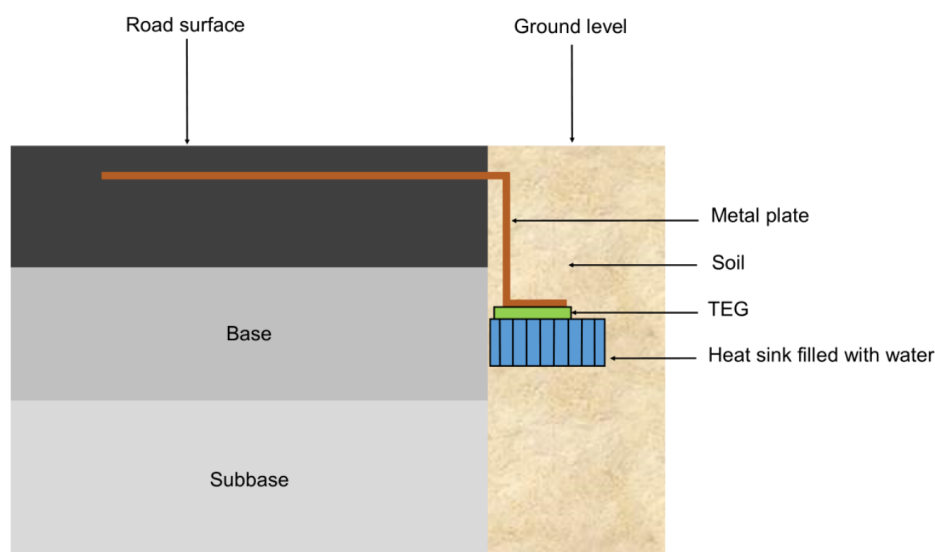


Figure 3. Thermoelectric harvester prototype [48]

The innovative work by Tahimi et al. [7] proposed a unique setup for an energy harvesting system, sharing some similarities with the studies conducted by Datta et al. [48] and Wei et al. [49]. Their system integrates a heat collector, a thermoelectric generator, and a coolant module. Notably, in comparison to Datta’s system, Tahimi et al.’s design replaces the heat sink with a coolant module incorporating phase change materials, an aerogel cover, a foam box, and a PVC box. Additionally, Tahimi et al. [7] used Finite Element Method (FEM) simulations to examine component characteristics and determine the optimal design of the prototype. The outcomes revealed that the L-shaped plate, with a width of 200 mm, exhibited the most substantial temperature gradient, leading to a heightened energy harvest. Significantly, their study underscored the enhanced performance of the system upon integrating a phase-changing heat sink within the coolant module. This finding contributes valuable insights to the optimization of thermoelectric energy harvesting systems embedded in pavement structures.

In the design of a thermoelectric harvester, material selection plays a crucial role. Twaha et al. [50] conducted a review focusing on the materials and performance of thermoelectric technology. The figure of merit (ZT) serves as an indicator of material performance, with a higher ZT corresponding to increased thermoelectric efficiency. To achieve a higher ZT , it is essential to have lower thermal conductivity and higher electrical conductivity in the material. The study revealed that the ZT values for these materials typically hover around 1.0.

1.2.3. Piezo-thermoelectric harvesting systems: On road pavement, there are several technologies to exploit mechanical and thermal ambient energy sources. The choice of technology to use depends on its features and applicability to the road pavement. Gholikhani et al. [9] conducted a review on these harvesting technologies. In their work, the advantages, disadvantages, and output of roadway harvesting technologies were evaluated. It was found that piezoelectric and thermoelectric harvesters are more promising for real-world implementation than other methods. Even if the harvester power is lower than that of a photovoltaic system, they can be adapted and installed more efficiently for roadway applications. Papagiannakis et al. [24] also conducted a review on energy harvesting technologies from roadways. Their work reported that piezoelectric harvesters have a wider power density according to voltage compared to other technologies. Guo and Lu [47] confirm the efficiency of piezoelectric and thermoelectric systems for road applications. According to the existing review and the application of the harvester, the combination system proposed in this work will exploit piezoelectric harvesters to collect vibration energy and thermoelectric harvesters to collect thermal energy available on roads.

The innovation proposed in this work consists of combining both piezoelectric and thermoelectric harvesting systems. Several approaches have been adopted to arrive at a combination of thermoelectric and piezoelectric technologies in the literature:

- Numerical simulation: Wu and Yu [51] conducted a numerical simulation. Their research featured a design incorporating a $4\text{ cm} \times 4\text{ cm} \times 0.5\text{ cm}$ aluminum plate attached to a 1 m-long aluminum rod. To minimize heat exchange with the asphalt, the rod was wrapped in a 590 mm-long heat insulator. The investigation included a systematic examination of various parameters aimed at optimizing the harvester's conception. For faster computing, it was also assumed that horizontal geological layers had uniform properties. This allowed for a 2D simulation that kept the accuracy of the design while speeding up the computing process.
- Electronic Simulation: Yoon et al. [52] conducted electronic simulation of a dual pile-up resonance energy harvesting circuit crafted to effectively extract energy from both a piezoelectric transducer and a thermoelectric generator. Their harvester functions in a dual pile-up mode, leading to an enhancement in power extraction, and in a boost converter mode, attaining a commendable 75% conversion efficiency. Li et al. [53] also worked on an electronic simulation of a piezo-thermoelectric harvesting system focused on parallel synchronized switch harvesting on an inductor (parallel SSHI). Dessai et al. [54] utilized maximum power point tracking (MPPT) for their simulation.
- Experimental prototype: Oh et al. [55] proposed a hybrid system to harvest human motion and heat energy. They achieved a flexible hybrid energy harvester that boosts power using thermoelectric and piezoelectric conversions. It enables sustainable energy harvesting by gathering energy from curved surfaces and low-frequency kinetic motion. The average power density was $28.57\ \mu\text{W}/\text{cm}^2$. Chen

et al. proposed the combination of these two systems [56]. In their study, the thermoelectric generator was used to enhance the piezoelectric harvester. The works of Jella et al. [57] were focused on the design of a single structured thermoelectric-piezoelectric-solar energy harvesting prototype. Organic-inorganic lead halide perovskite (MAPbI₃) is the main material used in their work. The proposed device can work as a piezoelectric harvester, a thermoelectric harvester only, or a photovoltaic harvester. The prototype can deliver 1.47 V and 0.56 μA .

However, most of the reported works on the combination of thermoelectric and piezoelectric for harvesting energy are not applied on the road [14]. Very few references have reported this combination on the road:

- The work of Mujaahid et al. [15] combined thermoelectric and piezoelectric systems to harvest mechanical and thermal energy on road surfaces. An experimental prototype was developed for this purpose. Laboratory experimentation on the thermoelectric harvester showed a maximum power of 1.55 *mW* for 6 hours of harvesting time, and the piezoelectric harvester produced 9.83 V for a stress of 235.04 *kPa*.
- Pacis et al. proposed to combine these two technologies on road surfaces [58]. The vibration from passing vehicles and the heat from solar radiation were transformed into electrical energy and produced a maximum power of 4.33W. Their work also proposed a MATLAB simulation of the system.

These hybrid road energy harvesters are based on an experimental prototype and a numerical simulation of the harvesting system. Our work is based on the proposition of an electronic model of the combination of thermoelectric and piezoelectric harvesting systems. A classical electronic model of a thermoelectric generator will be combined with a classical electronic model of a piezoelectric generator to achieve a hybrid harvesting system model. Then, a low-cost experimental prototype is conceived to validate the proposed model, which is designed for road application.

To summarize, there are still a few papers dealing with thermoelectric harvesting technologies and more dealing with piezoelectric in road applications. However, there are limited studies regarding the combination of the two technologies in road pavement applications. First, most existing studies in energy harvesting are in the laboratory prototype stage. There has not yet been a full-scale implementation of these technologies on road pavements. Some harvesting power limitations are already encouraging research on compensation and adaptive solutions to highlight the application of energy harvesting techniques. By proposing a new experimental prototype and model for the combination of thermoelectric and piezoelectric harvesting systems, this work will contribute to the advancement of this field.

2. Materials and Methods

2.1. Objectives

The main objective of this new experimental combination prototype is to remedy the intermittency problem of a single energy source. Existing research on energy harvesting from road pavements focuses on a single type of ambient energy: solar radiation, mechanical energy from passing vehicles, geothermal, rainwater, or wind energy [59]. However, if one source is not available, the whole production system will remain inoperative. That is the case during the night for solar energy exploitation, or when road traffic decreases for mechanical energy exploitation. In these cases, a power accumulator could be used to store the energy collected during the production phase, followed by restituting this energy when the sources are not available. However, the optimum case is to have permanently, if possible, an available energy source.

The second objective of this new experimental prototype is to exploit the 3-3 mode (the deformation of the piezoelectric material is parallel to its polarity) of a piezoelectric transducer. The 3-1 mode, in which the piezoelectric material deforms in a way that is perpendicular to its polarity, is the most common way to use resonant vibration harvesters that have a cantilever beam. But as seen in [60] and [61], the 3-3 mode allows transforming higher levels of mechanical energy into electrical energy. Most of the piezoelectrical harvesters (PZT-5, PZT-5A, $BaTiO_3$, PZN-7%PT) have a higher piezoelectric constant d_{33} in $[C/N]$. While only PVDF has a higher piezoelectric constant d_{31} [60] and [61]. The proposed experimental prototype will exploit this higher piezoelectric constant in the 3-3 mode to harvest the maximum mechanical energy. The difference between the 3-3 mode and the 3-1 mode is shown in Figure 4.

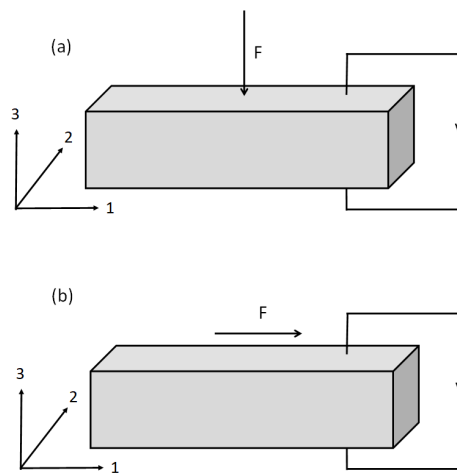


Figure 4. Piezoelectric modes: 33-mode (a) and 31-mode (b)

The third objective of this research project is to increase the harvesting system's output power. As stated at the beginning of this section, the primary objective of combining two energy sources is to solve the intermittent problem. However, the

harvested energy could be enhanced if two sources of energy are combined. This case is true when these two ambient sources are available simultaneously. For instance, when the solar radiation is high enough and there are high traffic volumes on the road. Then, instead of only solving the intermittency problem, mechanical and thermal energy can be collected simultaneously. Thus, the total harvested energy is enhanced, which is the third objective of this work.

2.2. Designing the experimental new prototype

To collect ambient energy available along road pavements, this work proposes to combine a thermoelectric energy harvester with a piezoelectric energy harvester. Thus, the prototype consists of two main parts: a part dedicated to harvesting thermal energy and another part dedicated to harvesting mechanical vibration energy.

First, the thermal harvester consists of a copper plate. This copper plate is embedded into the asphalt concrete layer. The role of this copper plate is to transport the heat from the asphalt surface to the thermoelectric generator. Copper is widely used because of its high thermal conductivity: 394 W/mK at $20 \text{ }^\circ\text{C}$ [62].

In their experiment, Jiang et al. [63] showed that the asphalt surface and the embedded copper plate had different temperatures depending on the depth of the copper plate. Due to heat loss through the asphalt layer, when the plate is deeper, the temperature difference is greater. Embedding the plate at 20 to 30 mm depth results in a temperature difference of temperature of about 3 to 4 $^\circ\text{C}$. According to the studies by Jiang et al. [63], this plate depth did not compromise the pavement performance; nevertheless, additional research and longer testing under repetitive load are needed to confirm the structural integrity of the road. It is assumed that these values are acceptable to ensure the integrity of the road structure.

A $40 \text{ mm} \times 2 \text{ mm} \times 300 \text{ mm}$ L-shaped copper plate is used and insulated with an isolation box made of polystyrene to minimize heat loss during the transportation of the heat to the thermoelectric generator. The polystyrene has a low thermal conductivity; it may vary from 0.032 W/mK to 0.045 W/mK [64]. Then, a thermoelectric generator is bonded to the edge of the copper plate.

Basically, through the Seebeck effect, the thermoelectric generator exploits a temperature gradient to generate a direct voltage. It transforms thermal energy into electrical energy. As the thermoelectrical generator exploits the temperature gradient, there is a hot side and a cold side. The hot side consists of the side connected to the copper plate, while the cold side consists of the other side connected to a heat sink.

The heat sink is generally made of aluminum and is used to absorb the heat and maintain the temperature gradient between the hot and cold sides of the thermoelectric generator. However, without proper cooling, this heat sink could also get heated because the heat flux is transferred from the hot side of the thermoelectric generator to its cold side. Thus, the cooling fins of the heat sink will be filled with Phase Change Material (PCM). Tahimi et al. [7] proposed this technique to maintain the cold side

of the thermoelectric generator at 18 °C. The principle of a Phase Change Material is to absorb or release latent heat. This phenomenon occurs when the Phase Change Material is in a transition of its physical state (liquid to solid or solid to liquid) [65] under a specific temperature range (generally from 10 °C to 80 °C). The properties of such material allow for maintaining the temperature of the heat sink. Then, Aerogel covers the external surface of the heat sink. This material is also proposed in the thermoelectric harvester of Tahimi et al. [7] due to its insulation properties (0.012 W/mK). Finally, the external surface of the Aerogel is also covered by a polystyrene insulation box to minimize heat exchange with the external environment.

The proposed piezoelectric harvester is a new prototype of a resonant vibration harvester. It will exploit the 3-3 mode of a piezoelectric element, which converts higher mechanical energy into electrical energy (Paragraph 2.1). First, the prototype consists of a mass, springs, and piezoelectric transducers. The principle consists of matching the vibration frequency of the passing vehicles to the vibration frequency of the harvester system. In this case, a resonance phenomenon occurs, and the vibration reaches its maximum amplitude. Then, under a high-amplitude vibration, the piezoelectric transducers produce more electrical energy. In principle, the maximal electric charge (in a short circuit) generated by the piezoelectric transducer is proportional to the force applied to it according to the relation $Q = F \times d_{33}$. Where Q (in C: Coulomb) is the electric charge; F (in N) is the applied force; and d_{33} (in C/N) is the piezoelectric charge constant in 3-3 mode, which is specific to the piezoelectric transducer.

On the other hand, the maximal electrical voltage (in an open circuit) generated by the piezoelectric transducer is also proportional to the applied force, as in the relation $V = \frac{F \times g_{33} \times e}{L \times W}$. Where g_{33} (in m^2/C) is the piezoelectric voltage constant in 3-3 mode, e (in m) is the thickness, L (in m) is the length, and W (in m) is the width of the piezoelectric element. In the "mass + spring + piezoelectric" system, the force applied to the piezoelectric element is higher when the amplitude of the vibration of the "spring + mass" system is at its maximum value.

The mass represents a solid mass "m" (in kg), which will be used to tune the harvester frequency. Then, if we assume that it is a permanent, non-damped vibration, the frequency can be tuned using the relation $f = \frac{1}{2\pi} \sqrt{\frac{k}{m}}$. Where f (in Hz) is the natural frequency of the system; k (in N/m) is the spring constant of the system; and m (in kg) is the mass of the system. As we can see, the natural frequency of the system depends on the spring constant k and the mass m . The objective is to reach the phenomenon of resonance, and maximize the force applied to the piezoelectric transducer. Song et al. [66] researched road vibration energy harvesters. Their paper reported that there is a correlation between the speed of passing vehicles and the road vibration frequency, which is a linear correlation [66]. Thus, if the average speed of passing vehicles (and the road vibration frequency) is determined, the natural frequency of the harvester system can be tuned with the mass m to cause the resonance phenomenon.

To minimize the loss of mechanical vibration energy during the harvesting process, the proposed piezoelectric harvester should be installed near the pavement surface. During the designing process, the performance of the pavement surface must be taken into consideration and the proposed harvesting system should not affect this performance. For this purpose, an example of implementation is proposed in this work in Figure 5.

In this configuration, the copper plate is embedded in the asphalt pavement. The thermoelectric harvesting system is outside the asphalt pavement and could be covered in soil. The piezoelectric harvesting system could be placed in a protective box and installed on the surface of the asphalt pavement. If the piezoelectric system is embedded inside the asphalt pavement structure, the vibration could be attenuated by the structure. This configuration allows the maximum mechanical vibration energy to be harvested without impacting the pavement surface performance. If this arrangement is installed at the roadside, the safety of the roadway should not be affected.

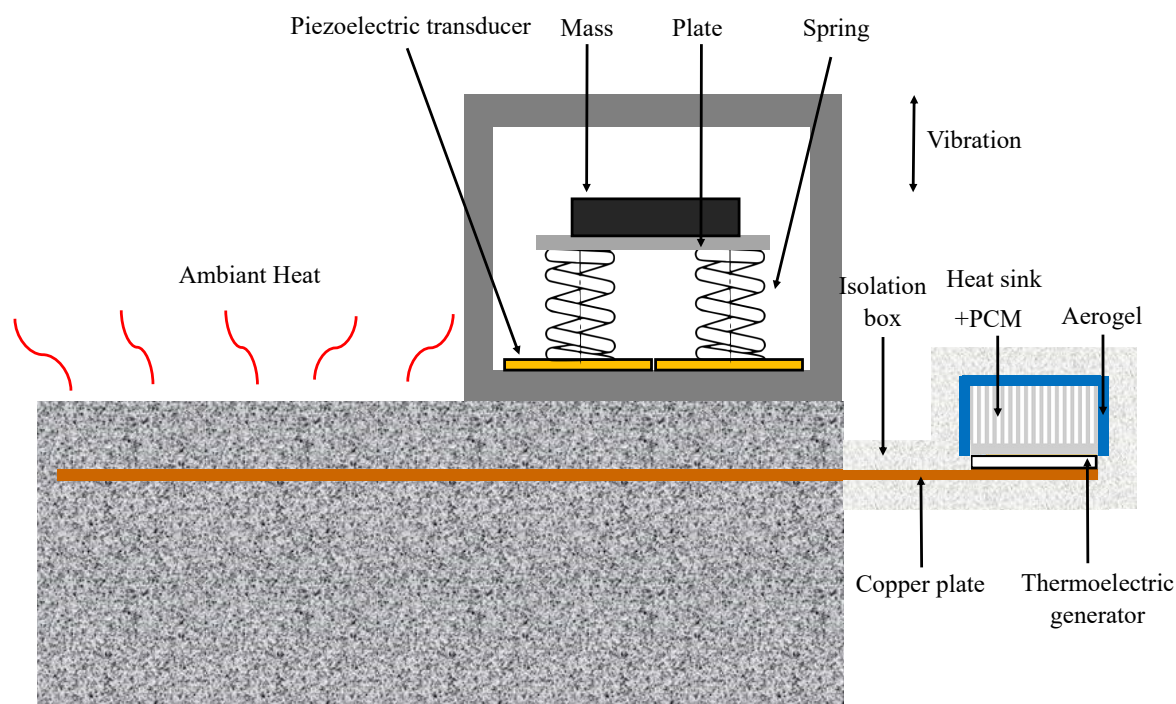


Figure 5. Implementation of the new prototype

In addition, the hybrid harvesting system will be exposed to high temperatures during the day. Consequently, some consideration should be given to the effect of temperature in the design step of the prototype. Piezoelectric materials are sensitive to temperature variations. Exposure to high temperatures affects the piezoelectric coefficients and electric properties, as well as the conductivity and dielectric properties

of the material. It will also conduct material degradation [67], [68]. To prevent these negative effects of temperature, we propose to add thermal insulation inside the cover of the piezoelectric device when the configuration in Figure 5 is adopted. Then, the cover will protect the device from shocks and high temperatures.

Thermoelectric generators are also impacted by high-temperature exposure. High temperature exposure accelerates structural degradation (oxidation and corrosion) and electrical degradation of the thermoelectric generator [69], [70], [71]. To address these issues, the thermoelectric generators will not be embedded directly under the road but will be relocated under the roadside. The ambient and latent heat through the thickness of the road will not directly affect the device. However, the use of a copper plate as a heat conveyor allows us to exploit this high temperature and harvest it. The use of an appropriate cooling system in the cold face of thermoelectric generators will also address the effect of prolonged exposure to high temperatures and enhance the harvested energy. For that purpose, we suggest using a passive cooling system through a heat sink, PCM, and Aerogel as proposed in the configuration in Figure 5.

2.3. Laboratory testing

This section describes the laboratory testing regarding the proposed prototype. The main objective of these laboratory tests is to evaluate the potential of the combination of the two systems (thermal and mechanical). The prototype described in paragraph 2.2 will be exploited without embedding it in an asphalt pavement structure. In this paper, the effect of the asphalt pavement structure [72] is not yet studied but will be analyzed in future work. The main purpose of this work is to introduce the feasibility of combining the thermoelectric and piezoelectric harvesting systems in a road pavement application. During the laboratory testing of the prototype, the optimization of the system was also not addressed at this stage of the research. The optimization will be addressed in future work due to a more specific material (e.g., Aerogel for the heat sink filling to keep it cold without air circulation).

The steps of the laboratory testing consist of simulating the thermal and mechanical solicitations applied to the harvesting system. Then, collect and combine the electrical output of the two harvesting systems. Finally, to analyze the electrical outputs and establish the relationship between the input solicitations and the electric outputs.

2.3.1. Fabrication process of thermoelectric device: The low-cost laboratory prototype of the thermoelectric harvester consists of :

- heat source: a conventional electric heater
- heat transporter: an aluminum tube
- thermoelectric generator: a TEC1-12706 Peltier plate
- cooling system: a heat sink with cooling wings

The appropriate material for heat transportation is copper because of its high thermal conductivity. However, the main heat source used during this experimentation was a conventional electric heater. A high-temperature source is needed to run the laboratory testing. To eventually avoid damage to the electric output cable of the thermoelectric generator, the heat needed to be transported away from the direct heat source of the conventional electric heater. Due to the high temperature, the use of polyester to insulate the copper plate may not be suitable for this configuration of the experimentation. The copper plate is not insulated, and instead of using a flat copper plate (where more heat variations may occur during a short period of time), an aluminum tube was used to transport the heat to the hot face of the TEG with a better pseudo-steady temperature.

The external dimension of the aluminum tube is $40mm \times 20mm \times 300mm$ with a thickness of $2mm$. This heat transportation also allows to maintain the temperature of the hot face of the thermoelectric generator at a pseudo-constant value, especially when the thermostat of the heating plate is switching and when temperature inertia appears.

During this experimentation, the heat sink was exposed to ambient air in order to maintain the cold face of the thermoelectric generator. The dimensions of the heat sink and the thermoelectric generator were met at $40mm \times 40mm$. In this configuration, it is assumed that the temperature on the cold face of the thermoelectric generator is uniform and does not alter the value of the measured temperature gradient.

The thermoelectric generator is the TEC1-12706 model from the Hebei I.T. thermoelectric cooler. Its dimension is $40mm \times 40mm \times 3.9mm$. In the case when more TEGs were used in laboratory testing, the TEGs could be arranged physically in parallel to harvest the thermal energy along the road and electrically in series to enhance the electric outputs. Table 2 gives manufacturer information about the thermoelectric generator, and the datasheet of the module can be found in [73].

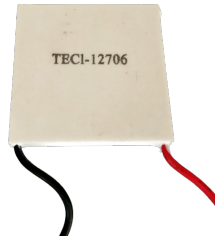
Description (units)	Value
Device	Thermoelectric cooler
Picture	
Manufacturer	Hebei I.T.
Model number	TEC1-12706
Dimension (mm)	40 x 40 x 3.9
Delta Tmax (°C)	75
Max. Operating Temperature (°C)	138
Life expectancy (hours)	200000
I _{max} (Amps)	6.4
V _{max} (Volts)	16.4

Table 2. Manufacturer information - Thermoelectric generator [73]

Finally, a heat sink of $40\text{mm} \times 40\text{mm} \times 30\text{mm}$ is bonded to the cold side of the thermoelectric generator. The electrical output of the thermoelectric generator is directly measured by the electric wires. Figure 6 shows the laboratory prototype of the thermoelectric harvesting system.

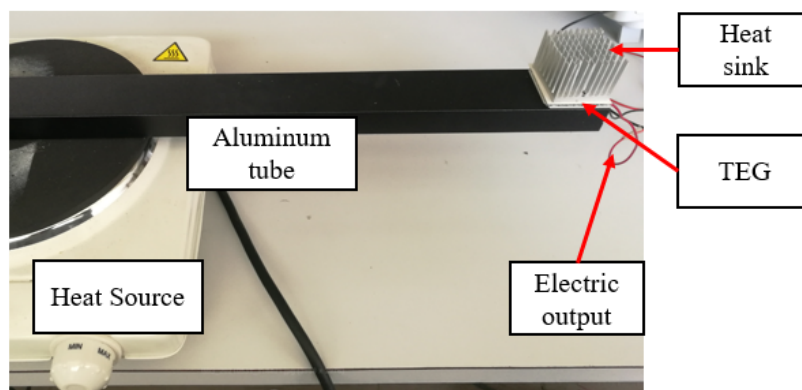


Figure 6. Laboratory prototype of the thermoelectric harvester

2.3.2. Fabrication process of piezoelectric device: The laboratory prototype of the piezoelectric harvester consists of a "mass + spring + piezoelectric" system composed of the following devices:

- mass : a combination of seven cylindrical tip masses to make a total of 550g
- spring: four helical springs installed on the four corners of a plexiglas plate

- piezoelectric: four KPSG100 piezoelectric transducers

The tip mass used for this laboratory prototype is a combination of small weights classified in two categories: 50g and 100g. This configuration allows tuning the natural frequency of the system by adding or removing weights. In the experiment, four weights of 100g and three weights of 50g were used to tune the natural frequency of the harvesting system. Thus, the total mass is about 550g. These weights are bonded together with double-sided tape. These weights rest on a plexiglass plate of $100mm \times 100mm \times 4mm$ of dimension for 5g of weight.

A plexiglass plate is used for its resistance and its small weight. Thus, this material could support the vibration of the mass without impacting the tuning of the system frequency because of its negligible mass. The weights are also bonded to the plate with double-sided tape. The plexiglass plate rests on four identical springs. These springs are positioned at the four corners of the plexiglass plate.

This configuration allows for uniformly distributing the load of the weights to the four springs and getting synchronous vibrations. The spring constant of a single spring is $k_1 = 680 \text{ N.m}^{-1}$. When four identical springs are exploited in parallel, the total spring constant of the equivalent spring is the sum of the spring constants of each spring, which means $k = k_1 + k_2 + k_3 + k_4 = 2720 \text{ N.m}^{-1}$. Then, these springs are bonded to four identical piezoelectric transducers.

The piezoelectric transducers used in this laboratory are KPSG100 models from KINGSGATE. Table 3 gives manufacturer information about the piezoelectric transducer. Their datasheet is also available in [74]. The whole assembly is then installed on a wooden board to avoid any interaction with the piezoelectric transducer in a case of metallic board.

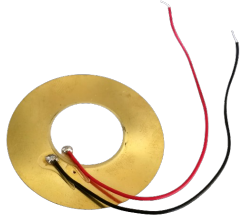
Description (unit)	Value
Device	Piezoelectric speaker
Picture	
Manufacturer	Kingstate Electronic
Model number	KPSG100
Dimension - Diameter x thickness (mm)	50 x 2.2
Vmax input (Volts)	30
Operating Temperature range (°C)	-20 to +70
Resonant frequency, only for piezoelectric element without wire (Hz)	1200
Resonant impedance (Ohm)	3500
Weight (g)	3

Table 3. Manufacturer information - Piezoelectric harvester [74]

The electric outputs of the piezoelectric transducers are directly available for connection through the electric wires. They are connected in series to enhance the output voltage of the system. The whole piezoelectric harvesting system is mounted on a wooden structure, which is subjected to constant vibration. Figure 7 shows the configuration of the laboratory prototype of the piezoelectric harvesting system.

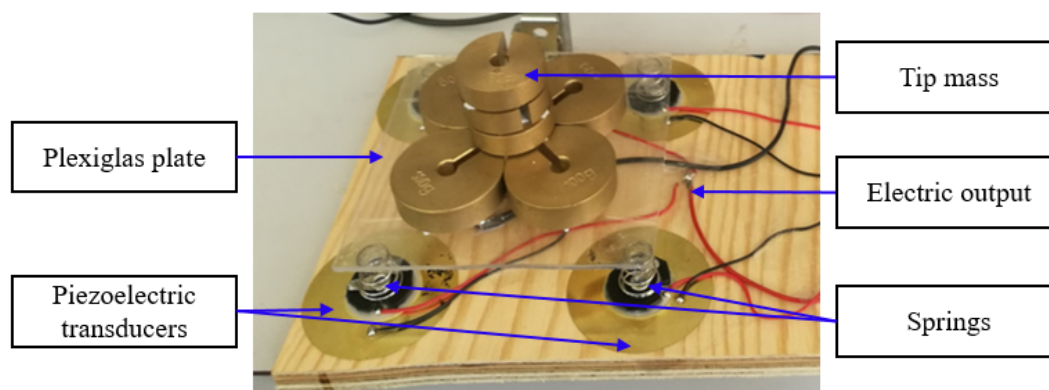


Figure 7. Laboratory prototype of the piezoelectric harvester

2.3.3. Data acquisition and measurement: The thermoelectric harvesting system and the piezoelectric harvesting system are now set up for laboratory testing. In order to run the experimentation, measure, and collect electrical outputs from the harvesting system, we have used the following devices:

- a servo motor controlled by Adruino
- a DC voltage source
- a full bridge rectifier circuit
- a Campbell data logger
- a Keysight oscilloscope

Figure 8 shows the disposition of the laboratory test of the piezo-thermoelectric harvesting system.

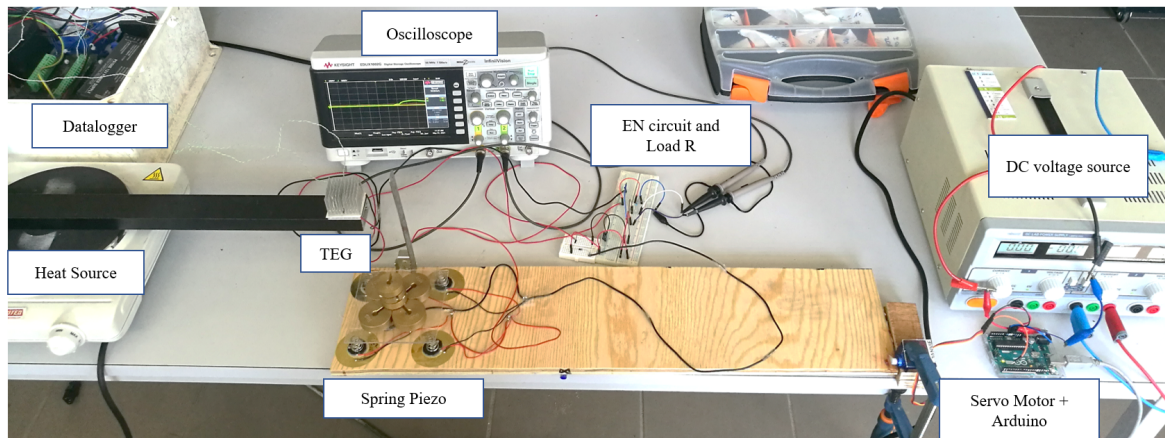


Figure 8. Laboratory testing disposition

The heat source of the thermoelectric system is the heat plate, while the vibration source of the piezoelectric system consists of a servo motor controlled by an Adruino Uno microcontroller. A DC voltage source is used to supply the Arduino microcontroller and the servo motor. The wooden structure has a pivot near its middle, and the servo motor hits the free end of that structure with a regulated frequency. The other end of the structure contains the piezoelectric system, which is vibrating through the solicitation of the servo motor by the pivot.

The thermoelectric harvesting system produces a direct DC voltage, while the piezoelectric harvesting system produces an AC voltage due to the periodic vibration solicitation. A full-bridge rectifier circuit is used to transform this AC voltage into a DC voltage. The rectifier circuit is mounted on an electronic test board. The output wires of these two systems are then connected in series on that electronic test board. An emplacement for load resistance is available to test the combined system under different values of resistance.

For data acquisition, a data logger is used to collect the temperature variation on the two sides of the thermoelectric generator. The data logger is a Campbell Scientific CR6, and the temperature was probed using calibrated thermocouples, which are connected directly to the datalogger.

The heat source (heating plate) warms the aluminum tube. The aluminum tube is connected to the hot side of the thermoelectric generator. A thermocouple is bonded

with thermal glue between the aluminum tube and the hot side of the thermoelectric generator to probe its temperature. Also, another thermocouple is bonded between the cold side of the thermoelectric generator and the heat sink to probe the lower temperature.

A "Keysight InfiniiVision EDUX1002G Digital Storage" oscilloscope is connected to the electrical outputs of the combined system. This oscilloscope measures and displays the evolution of the voltage across the resistor. Measurement data and graphs on the display screen are saved on a computer or in external memory for further processing. Figure 9 shows an example of graph saved from the oscilloscope. The voltage collected from piezoelectric harvester without rectifier is colored in orange while the harvester with rectified circuit is in green.

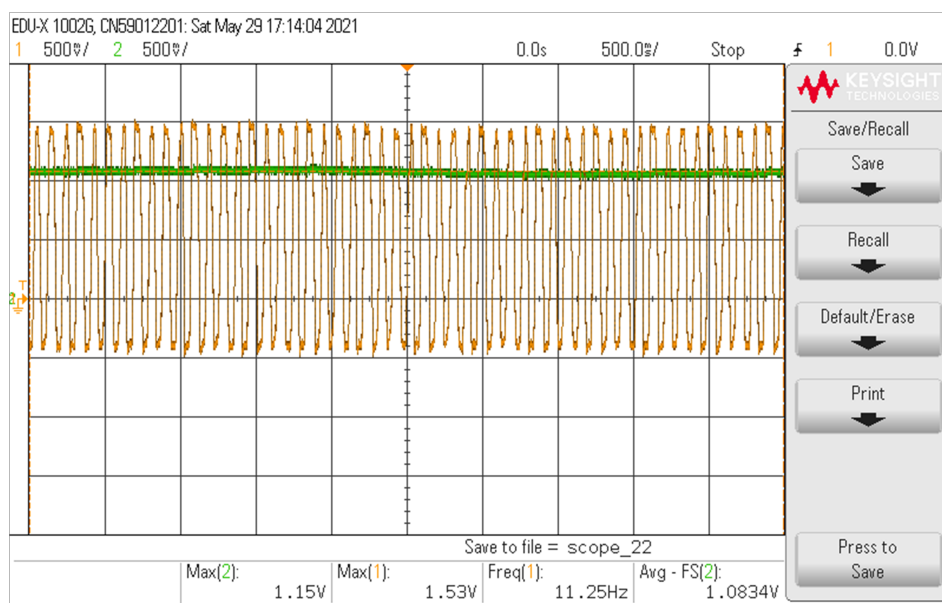


Figure 9. Oscilloscope graph - piezoelectric harvester voltage without and with rectifier circuit

3. Results

3.1. Thermoelectric and piezoelectric model

3.1.1. Thermoelectric model: A thermoelectric generator is based on the Seebeck effect. It converts the temperature gradient directly into electrical voltage. This gradient temperature is located between the two faces of TEG: one face is exposed to a higher temperature, and the other face is exposed to a lower temperature.

A TEG consists of N pairs of p-type and n-type semiconductor elements. These semiconductor elements are electrically connected in series to obtain a higher voltage and more electrical power. Also, they are thermally arranged in parallel so that each junction is exposed to the same thermal gradient. Two ceramic plates cover these semiconductor elements on either side, and it is these plates that will be exposed to the

temperature difference. In this way, heat is transferred from the hot side to the cold side.

The basic structure of a TEG is shown in Figure 10. It is formed by the combination of two pairs of p-n semiconductor elements with an electrical charge (resistor) connected across them. When the temperature on the hot side is higher than the temperature on the cold side, heat flows through the TEG. This heat flow causes the charge carriers (electrons and holes) to move in opposite directions. This displacement then causes an electric current I to flow through the load R_L connected to the output of the TEG [75].

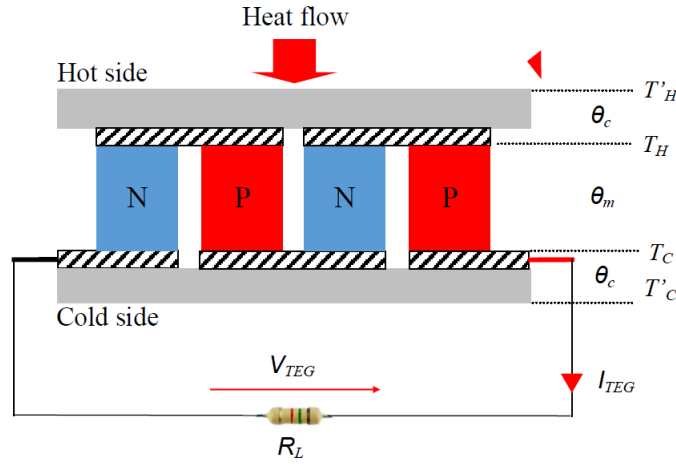


Figure 10. The basic structure of TEG [76]

The electrical outputs of the TEG are the generated voltage V_{TEG} (in V), the electrical load applied to the TEG R_L (in Ω), and the current I_{TEG} (in A) flowing through the load R_L

The parameters that define a TEG are:

- The total Seebeck coefficient of the TEG

$$\alpha_{TEG} = N(\alpha_p - \alpha_n) \quad (1)$$

where N is the number of p-n pair semiconductor elements in the TEG, α_p is the Seebeck coefficient of the p semiconductor element, and α_n is that of the n semiconductor element. item The internal thermal resistance θ_m (in K/W) of all N pairs of p-n semiconductors.

- The contact thermal resistances θ_c (in K/W) of the plate on the hot side and the plate on the cold side.
- The external temperature was applied to the hot side plate of the TEG T'_H (in K).
- The external temperature was applied to the plate on the cold side of the TEG T'_C (in K).
- The internal temperature was applied across the p and n semiconductor elements on the hot side of the TEG T_H (in K).

- The internal temperature was applied across the p and n semiconductor elements on the cold side of the TEG T_C (in K).

Siouane [76] proposed a TEG model that includes these thermal resistances, θ_c . His study is based on the development of a TEG model as a generic Thevenin equivalent circuit. The hypothesis is that the system is subject to constant temperature gradient conditions. The Thevenin equivalent circuit is then an equivalent DC voltage source in series with an equivalent resistor, as shown in Figure 11.

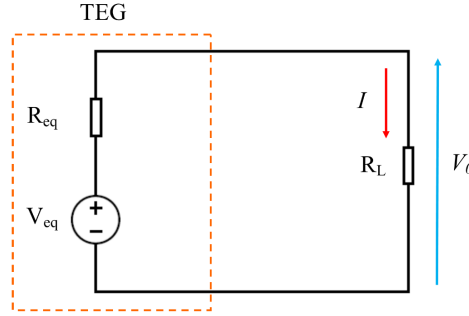


Figure 11. Generic equivalent Thevenin circuit for a TEG under a constant temperature gradient [76]

According to this hypothesis, the equivalent voltage source V_{eq} (in V) is expressed by [76]:

$$V_{eq} = \alpha_{TEG} \Delta T' \frac{\theta_m}{\theta_m + 2\theta_c} \quad (2)$$

Where $\Delta T'$ is the external temperature gradient applied to the hot and cold side plates of the TEG such that:

$$\Delta T' = T'_H - T'_C \quad (3)$$

The equivalent resistance R_{eq} (in Ω) is expressed by [76]:

$$R_{eq} = R_E + \frac{\alpha_{TEG}^2 \theta_c \theta_m (T'_H + T'_C)}{\theta_m + 2\theta_c} \quad (4)$$

Where R_E (in Ω) is the electrical resistance, which includes the resistance of the p and n semiconductor elements as well as the resistance of the contacts used to connect the TEG to an electrical load. The total voltage received by the load resistance R_L is then expressed by:

$$V_0 = V_{TEG} = \alpha_{TEG} \Delta T' \frac{\theta_m}{\theta_m + 2\theta_c} - \left[R_E + \frac{\alpha_{TEG}^2 \theta_c \theta_m (T'_H + T'_C)}{\theta_m + 2\theta_c} \right] I \quad (5)$$

We can thus calculate the power supplied by the TEG and received by the resistance R_L via the following relation:

$$P_{TEG} = V_{TEG} \times I \quad (6)$$

$$P_{TEG} = \alpha_{TEG} \Delta T' \frac{\theta_m}{\theta_m + 2\theta_c} I - \left[R_E + \frac{\alpha_{TEG}^2 \theta_c \theta_m (T'_H + T'_C)}{\theta_m + 2\theta_c} \right] I^2 \quad (7)$$

Research regarding thermoelectric energy harvesting has a simplified equivalent electrical model [77], [78]. That simplification is made by including the effect of thermal resistances θ_c and θ_m in the Seebeck coefficient α_{TEG} . In this study, we will also assume that the effects of thermal resistance θ_c and θ_m are included in the Seebeck coefficient. In addition, we can assume that ΔT is the temperature gradient between the hot and cold sides of the TEG such that $T_H = T'_H$ and $T_C = T'_C$. Then, the voltage across a TEG can be formulated as:

$$V_{TEG} = \alpha_{TEG}\Delta T \quad (8)$$

This equation is used in the following studies to determine the behavior of a TEG, which is directly a DC voltage source per the temperature gradient between the two faces of the TEG. The Seebeck coefficient α_{TEG} represents the ratio between the potential difference generated and the gradient temperature where the two faces are exposed. This is the essential characteristic of a TEG.

In real-world road pavement conditions, the temperature begins lower in the morning, rises to a maximum in the middle of the day, and then falls at the end of the day. Seasonal variations influence temperature gradient changes as well. A higher amount of solar radiation conducts to a higher temperature on the asphalt surface during the summer, while a lower temperature is observed on the asphalt surface during the winter.

The intensity of solar radiation also depends on the location of the considered road pavement. The temperature gradients between the hot and cold sides of the TEG depend directly on the solar radiation on the road pavement, the quality of the heat transportation (copper plate and insulation), and the quality of the cooling system installed on the cold side of the TEG. According to the Seebeck effect, a change in temperature gradient affects linearly the power generation (Equation 8). A higher temperature gradient generates a higher power output on the TEG, while a lower temperature gradient produces a lower power output.

3.1.2. Piezoelectric model: Piezoelectricity can be defined as the property of certain materials (crystals, ceramics, polymers, or composites) that can become electrically polarized under the action of a force. If a force is applied, the mechanical stresses that appear in the material cause deformations of its physical structure. This deformation will cause the creation of electrical charges on the opposite faces of the piezoelectric material. The purpose of a PiezoElectric Generator (PEG) is to transform the mechanical energy caused by the action of a force into electrical energy. In general, in energy harvesting applications, a PEG exploits mechanical vibrations to transform them into electrical energy.

To model a PEG, the researchers take the example of a beam embedded on one side and having a mass on the other free side. The piezoelectric element is placed near the embedding, where the stress is maximum, to obtain the maximum energy. This configuration is commonly used in research for piezoelectric harvesting systems [79], [80].

Rendon-Hernandez et al. [81] also designed a similar cantilever system for a piezoelectric generator that is activated by a thermo-magnetic technology. The main objective is to tune the natural frequency of the harvesting system to match the frequency of the vibration source. Then, a resonance phenomenon appears, and a maximum amount of energy can be harvested from the piezoelectric transducer. To measure the output power of the harvesting system, an electrical resistance load is placed on the two electrodes of the piezoelectric material (Figure 12).

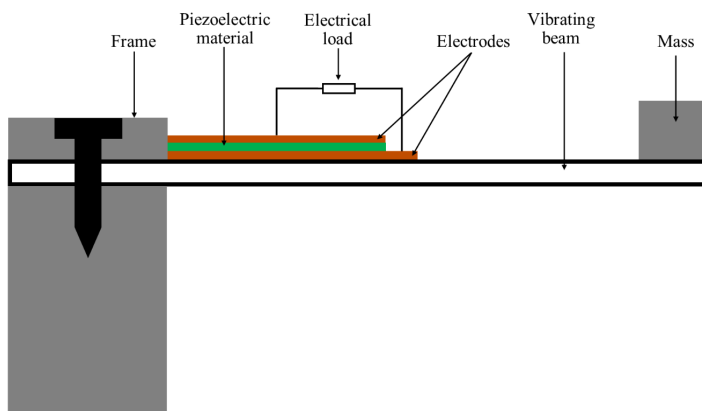


Figure 12. 3-1 mode piezoelectric energy harvesting device

This cantilever configuration exploits essentially the 3-1 mode of a piezoelectric generator. Thus, this configuration generates effective power if the piezoelectric material is suited for a 3-1 mode, such as Polyvinylidene Difluoride (PVDF). For other piezoelectric materials that are suited for a 3-3 mode, such as Lead Zirconate Titanate (PZT) or Barium Titanate (BaTiO₃), an original configuration is proposed to harvest the energy of these 3-3 mode materials and maintain the capability of existing models of a piezoelectric generator.

The proposed configuration consists of a tip mass placed on a spring system. The piezoelectric materials are then placed under this spring system. The piezoelectric materials rest on a vibrating frame. The source of the vibration is thus associated with the vibrating frame that induces a movement of vibration noted x . A schematic of the proposed configuration is shown in Figure 13.

As seen in Paragraph 2.2, the role of the tip mass is to tune the vibration frequency of the harvester system to converge to the vibration frequency of the mechanical vibration source as the relation $f = \frac{1}{2\pi} \sqrt{\frac{k}{m}}$ where k is the spring constant and m the mass of the tip mass. The objective is to approach the resonance phenomenon and enhance the vibration amplitude of the harvester system. The role of the spring is to maintain the vibration even if the source of mechanical vibration is gone. As the cantilever beam, it maintains the mechanical energy with the tip mass to keep soliciting the piezoelectric material and extend the duration of the harvesting process. The force applied to the piezoelectric materials is maintained sinusoidally by the action of that

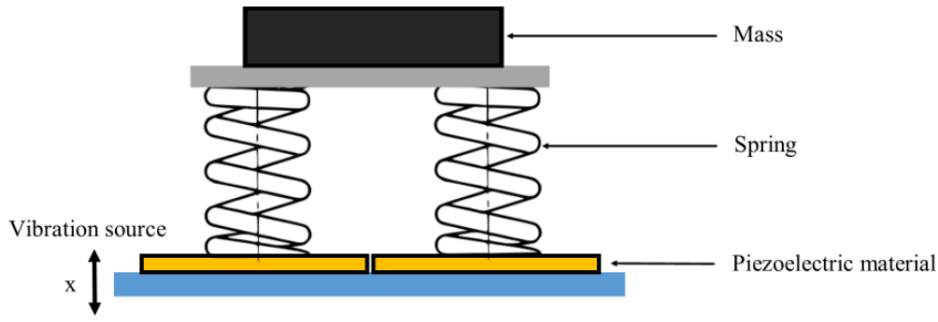


Figure 13. 3-3 mode piezoelectric energy harvesting device

spring.

Finally, the role of the piezoelectric material is to transform the mechanical vibration energy into electrical energy. One of the best advantages of using this mode is that the longitudinal piezoelectric effect (3-3 mode) is usually much larger than the transverse piezoelectric effect (3-1 mode).

Around the resonant frequency of the structure, most papers proposed an electro-mechanical model of the power generator [82], [83]. Thus, with the assumption of small displacement, the PEG can be modeled as a "mass + spring + damper + piezo" assembly. Thus, we can consider a forcing function $F(t)$ that is applied to the harvesting system. An effective mass is bonded to a spring, a damper, and a piezoelectric element characterized by an effective piezoelectric coefficient α_{PEG} and internal capacitance C_p . According to this mechanical model, Khalili et al. [16] proposed an electro-mechanical correspondence and an equivalent electrical model. Through this equivalent electrical scheme, Vasic et al. [84] proposed the equivalent scheme of PEG for the case of a mechanical excitation maintained at the resonance frequency (Figure 14).

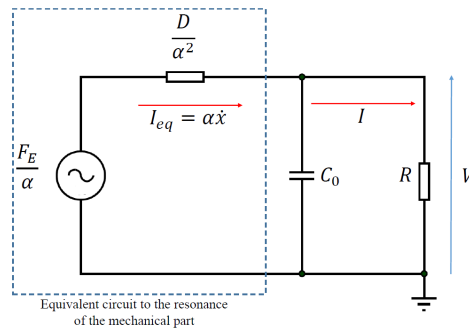


Figure 14. Equivalent circuit to the resonance [84]

Where:

- I_{eq} (in A) is the equivalent current which is the image of the vibration velocity
- \dot{x} (in m/s) is the vibration speed
- R (in Ω) is the electrical resistance which indicates the charge

The main objective of this study is to realize the coupling of a thermoelectric generator (TEG) with a piezoelectric generator (PEG). The hybrid system obtained will then be a piezo-thermoelectric generator (PTEG). As seen in Figure 11 the final voltage delivered by the TEG is a DC voltage. However, as shown in Figure 14, the final voltage delivered by the PEG is sinusoidal. To realize the coupling, it is necessary to rectify the output voltage of the PEG. Then, a rectifier circuit is installed at the output of the piezoelectric transducer, which consists of a diode bridge combined with a smoothing capacitor. To do this, the schematic in Figure 15 is proposed in the work of Vasic and Costa [84].

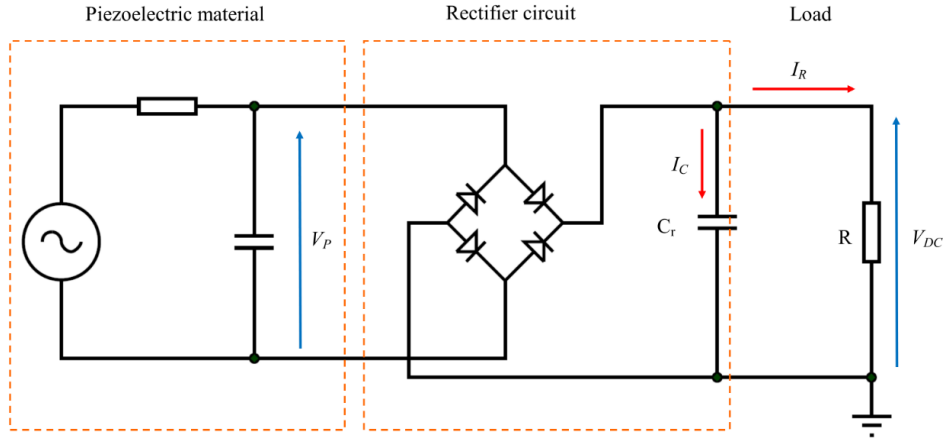


Figure 15. Voltage rectifier circuit [84]

Where:

- V_P (in V) is the sinusoidal voltage supplied by the piezoelectric element
- V_{DC} (in V) is the rectified voltage that supplies the load R

The expression for the rectified voltage is given by [84]:

$$V_{DC} = V_{PEG} = \frac{2R\alpha_{PEG}}{\pi + 2RC_0\omega_0} \cdot \frac{F_E}{D} \quad (9)$$

Where:

- F_E (in N) is the force applied to the piezoelectric element
- D (in kg/s) is the damping coefficient of the harvesting system
- α_{PEG} (in N/V) is the force factor of the piezoelectric element model
- R (in Ω) is the load resistance of the harvesting system
- C_0 (in μF) is the internal capacitance of the piezoelectric element model
- ω_0 (in rad/s) is the pulsation of the vibration of the harvesting system

And the expression of the supplied power is given by :

$$P_{PEG} = \frac{V_{PEG}^2}{R} = \frac{4R\alpha_{PEG}^2}{(\pi + 2RC_0\omega_0)^2} \cdot \frac{F_E^2}{D^2} \quad (10)$$

According to Equation 9, it is possible to maximize rectified voltage and, consequently, power by optimizing the resistance to be used. Thus, the optimal resistance corresponds to:

$$R_{opt} = \frac{\pi}{2C_0\omega_0} \quad (11)$$

Using this optimal resistance, we obtain the maximum power:

$$P_{max} = \frac{\alpha_{PEG}^2}{2\pi C_0\omega_0} \cdot \frac{F_E^2}{D^2} \quad (12)$$

Using the optimal resistance, we also obtain the maximum rectified voltage:

$$V_{DCmax} = \frac{\alpha_{PEG}}{2C_0\omega_0} \cdot \frac{F_E}{D} \quad (13)$$

Finally, we have the maximum rectified current:

$$I_{Rmax} = I_{PEG} = \frac{\alpha_{PEG}}{\pi} \cdot \frac{F_E}{D} \quad (14)$$

These equations are used in the following to describe the behavior of a PEG.

3.1.3. Piezo-thermoelectric model: This work proposes a hybrid energy harvesting system that collects ambient energy from the road. The ambient energies are generated by two distinct phenomena: the vibration from passing vehicles and the heat from the solar radiation on the road surface. The vibration from passing vehicles generates mechanical energy, and the heat from solar radiation on the road surface generates thermal energy. These two phenomena are totally independent on the road. There may be passing vehicles on the road, or not. The sun may be radiating the road surface during the day or not during the night. Piezoelectricity is typically associated with dynamic mechanical forces and can respond quickly to changes in pressure or vibration, while thermoelectricity relies on temperature differentials and tends to have slower response times.

These phenomena in the real world are dependent on climate and road traffic, resulting in significant variability. The suggested coupling model does not involve a time-varying equation. In order to establish and implement the model, it is necessary to gather data and examine the mean frequency generated by vehicles as they pass on the road. This average value will then be utilized in the model. The electronic representation of the piezoelectric harvester is only valid when it operates at resonance. Therefore, it is essential to determine the average frequency in order to establish the resonance frequency of the model. In order to incorporate the thermal aspect, it is necessary to examine the mean temperature fluctuation within the tar layer, which will be utilized in the model. The mean values will subsequently be employed to supply the electronic models of the piezoelectric and thermoelectric harvesters. Given that the coupling model incorporates both vibration and heat, its validity is contingent upon the simultaneous presence of both phenomena. Only under these specific conditions can the two mechanisms be combined to make the model valid. In real applications, since the phenomena are dynamic and totally independent, it is recommended to use a

storage system to store the energy from each source in order to exploit their intermittent availability. We will then have a hybrid energy-harvesting system instead of a coupled energy-harvesting system.

Other works deal with the optimization of the electronic model in order to maximize the energy recovered during coupling. The use of Synchronous Switch Harvesting on Inductor (SSHI) circuits is widely used in the literature for that purpose [53], [83], [85]. SSHI represents a method employed in piezoelectric energy harvesting systems to enhance power extraction efficiency. The principle involves the synchronous modulation of the electrical impedance connected to the piezoelectric element. Through periodic adjustments of the impedance, SSHI aims to optimize power transfer from the piezoelectric harvester to the load, thereby ensuring effective energy harvesting from mechanical vibrations or deformations. This approach serves to augment the overall efficacy of piezoelectric energy harvesting systems by facilitating impedance matching throughout the dynamic operation of the harvester. In a future investigation about optimization, the SSHI circuit can be applied to the proposed electronic model to improve and optimize the harvested energy. In real implementation, we propose to use a Battery Management System (BMS), which will manage the synchronization of the two systems through the integration of the calculation code of the SSHI circuit.

By coupling the TEG and the PEG, a greater amount of recovered energy is obtained. Therefore, placing these two generators in series provides for a higher output voltage. It was verified in the literature that series configurations generate a higher power density for hybrid harvesters. Zhou et al. [86] have designed a combination of PEG and TEG applied to a waste heat circulation pipe. In their study, series and parallel configurations have been tested, and it was reported that series configurations generate a power density of $55 \mu W.cm^{-1}$ while parallel connections release $19 \mu W.cm^{-1}$. Indeed, the TEG can be considered a DC voltage generator, and the PEG associated with a rectifier circuit can also be considered a DC voltage generator. By placing these two generators in series, we add their output voltage. The piezo-thermoelectric generator circuit is shown in Figure 16. It is made by putting together the equivalent Thevenin circuit of the TEG (Figure 11) and the rectifier circuit of the PEG (Figure 15).

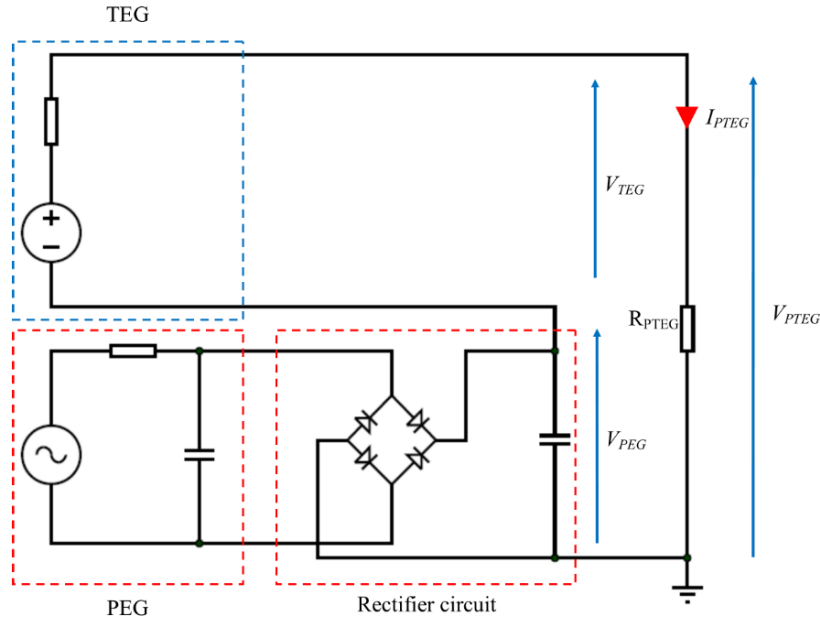


Figure 16. Equivalent circuit in series of the piezo-thermoelectric generator

Where:

- V_{TEG} (in V) indicates the current voltage supplied by the TEG
- V_{PEG} (in V) indicates the current voltage supplied by the PEG
- V_{PTEG} (in V) indicates the current voltage supplied by the combined system PTEG
- I_{PTEG} (in A) indicates the current intensity supplied by the PTEG
- R_{PTEG} (in Ω) indicates the electrical load at the output of the PTEG

The series configuration of the PTEG and the use of only one resistance load for the hybrid system conducted the study prior to an open circuit formulation. In the model proposed by Siouane [76], the open circuit voltage for the TEG is given by Equation 2. In this hybrid PTEG model proposition, the idea is to determine which parameters influence the electrical outputs directly in practical use. It will be assumed that the internal phenomena in the TEG (internal thermal resistance θ_m , contact thermal resistance θ_c , electrical resistance R_E) are not included in the TEG model for the coupling. Instead of that, Equation 8 will be used for the open circuit voltage, as the real Seebeck coefficient of the thermoelectric generator α_{TEG} could include all thermal and electrical resistance inside the thermoelectric material.

For the PEG, the output voltage is dependent on the resistance load (Equation 13). The open circuit voltage could be determined by turning the load impedance to match the internal impedance of the PEG by the relation $R_{opt} = \frac{\pi}{2C_0\omega_0}$ [87]. Thus, the open circuit voltage is determined by Equation 13. To avoid confusion about the symbols α , the authors denoted α_{PEG} (in N/V) the force factor of the piezoelectric element model and α_{TEG} (in V/K) the Seebeck coefficient of the thermoelectric element.

The total voltage generated by a series configuration is theoretically obtained by adding the output DC voltage from the TEG and the PEG as $V_{PTEG} = V_{TEG} + V_{PEG}$. The equivalent circuit of the combined system is simulated in a SPICE environment to understand the impact of the coupling on electric output. The proposed circuit is only valid for a constant temperature gradient (ΔT) for the thermoelectric system and a constant vibration under a resonance phenomenon for the piezoelectric system.

This work is about static phenomena. When the temperature gradient varies, the proposed circuit remains valid; the output voltage from the TEG may vary and influence the system's output power. The proposed equivalent circuit, however, will be invalid if the vibration is not constant and not subject to a resonance phenomenon. If these conditions are not met, the dynamic phenomenon may not be predicted by these circuits, and it needs additional research with experimental prototypes in a controlled environment.

3.2. Laboratory test case

The experimental prototype and the proposed electronic model are tested to ensure that the results are consistent. The various parameters of the piezoelectric and thermoelectric harvesting systems are established to allow the process to be repeated.

As described in Paragraph 3.1.1 regarding the thermoelectric model, it is assumed that the temperature gradient is constant. The model of the Seebeck effect can only be applied to that condition. Also, the piezoelectric model described in paragraph 3.1.2 is only applicable under certain conditions. It is assumed that the resonance frequency is the resonance of the structure; it is not influenced by the electrical circuit. Then, the electromechanical parameters of the system are described in Table 4.

Parameters (Units)	Values
C_0 (F)	0.000000134
α_{PEG} (N/V)	0.00008576
k (N/m)	2720
m (kg)	0.55
D (Ns/m)	1.1
f (Hz)	11.2
ω (rad/s)	70.37167544
α_{TEG} (V/K)	0.02898657

Table 4. The validation parameters.

For the piezoelectric harvesting system, there is the internal capacitance of the piezoelectric transducer C_0 , the force factor α_{PEG} , the spring constant k , the damping coefficient D , the resonance frequency f and the pulsation of the vibration ω . For the thermoelectric harvesting system, the main parameter is essentially the Seebeck coefficient α_{TEG} .

The results of the experiment and the simulation of the model are as follows: first, the thermoelectric harvesting system was tested separately. According to the Seebeck effect equation, the DC voltage from the thermoelectric system is directly dependent on the temperature gradient. As seen in table 4, the Seebeck coefficient is 0.0289 V.K^{-1} . During the experiment, the temperature gradient was defined with the heating plate. In the test case, the temperature gradient is $10 \text{ }^\circ\text{K}$. Then, different electric resistances were used to simulate the loading charge. Figure 17 shows the evolution of the output power under these different electric resistances.

As the Seebeck effect concerns the voltage of the thermoelectric generator directly, when the resistance is higher, the power becomes lower. The maximum amount of harvested power appears when the minimum value of resistance is utilized. Figure 18 shows the evolution of the voltage and the current within different resistors. It can be noticed that the output voltage of the prototype varies slightly. This is because of the regulation system of the heating plate, which tries to maintain the temperature at a constant value.

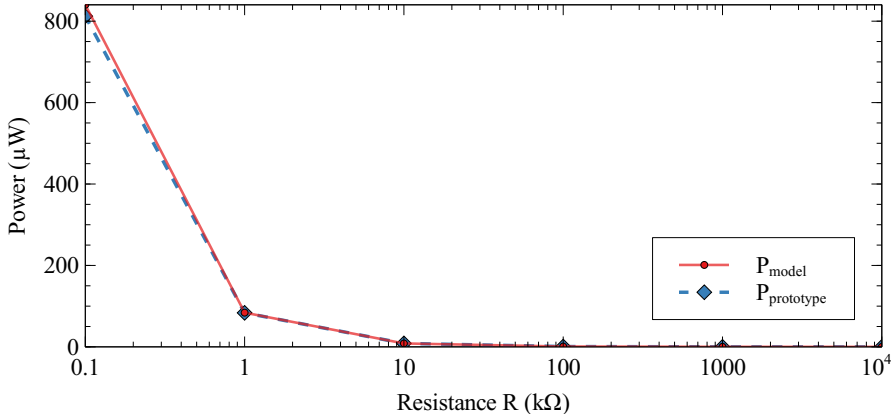


Figure 17. Thermoelectric harvesting system power

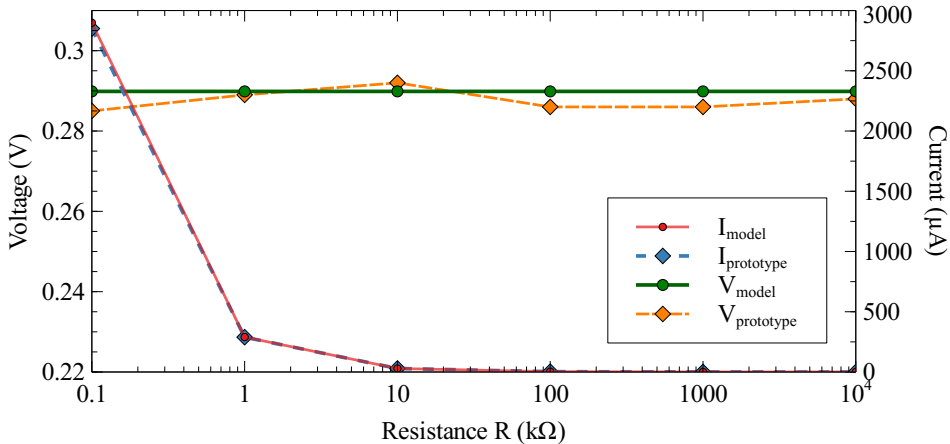


Figure 18. Thermoelectric harvesting system voltage and current

For the experiment with the piezoelectric harvesting system, the vibration frequency of the structure is tuned with the servo motor and the Arduino Uno controller card. That vibration frequency was tuned to match the natural frequency of the piezoelectric harvesting system. Finally, a frequency of 11.20 Hz was applied to the structure. With that frequency, the resonance phenomenon appears, and the displacement of the tip mass reaches 1 mm.

In the experiment of Song et al. [66] a direct correlation is observed between the speed of passing vehicles and the frequency of the harvester. According to their studies [66] a frequency of 11.20 Hz correlates to a vehicle speed of 66 $km.h^{-1}$. The load used in the piezoelectric harvester was adjusted to 0.55 kg to allow the system to vibrate at the resonant frequency, as seen in Table 4.

For the simulation of the model, the SPICE environment of ISIS Proteus was used. ISIS Proteus allows drawing the electronic equivalent scheme of the harvesting system. As for the earlier experimental process, different electric resistances were used during the simulation. These resistances vary from 0.1 $k\Omega$ to 50000 $k\Omega$. In contrast with the thermoelectric harvesting system, the piezoelectric one has an optimum value of resistance. to maximize the output power. The output power is low at lower resistance. The output power is then increased as the value of the resistance increases, up to a certain value of the resistance, when the maximum harvested power is achieved. Maximum power is obtained in a piezoelectric system at optimum resistance due to impedance mismatching. The process of designing source and load impedances to minimize signal reflection and maximize power transfer is known as impedance matching.

Impedance (Z) is a measure of the resistance to electrical flow, which is a complex value whose real component is resistance (R) and whose imaginary component is reactance (X). By definition, the impedance equation is $Z = R + jX$, in which j is the imaginary unit. In DC systems, reactance is nonexistent, so impedance and resistance are identical. Depending on the objective, the source in AC circuits should either equal the load or the complex conjugate of the load. Piezoelectric transducers are in the category of an AC source if the solicitation is constant. Finally, beyond this maximum power, even if the resistance value is increasing, the output power is decreasing.

Figure 19 demonstrates the evolution of piezoelectric harvester power. A small difference is noticed between the output power of the prototype and the model. This difference is mainly due to the vibration excitation, which can be influenced by the external environment. Some parasite vibrations could impact the harvesting system and induce slight measurement errors.

Figure 20 shows the variation of the voltage and the current under different resistance values. It can be noticed that the evolution of the current is the inverse of the evolution of the voltage. When the resistance is low, the current is at its maximum, while when the resistance is high, the current is at its minimum. The voltage is lowest when the resistance is low and highest when the resistance is high.

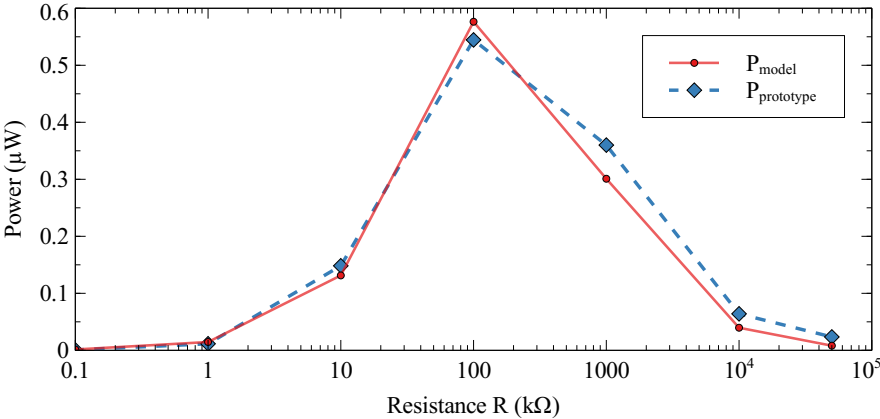


Figure 19. Piezoelectric harvesting system power

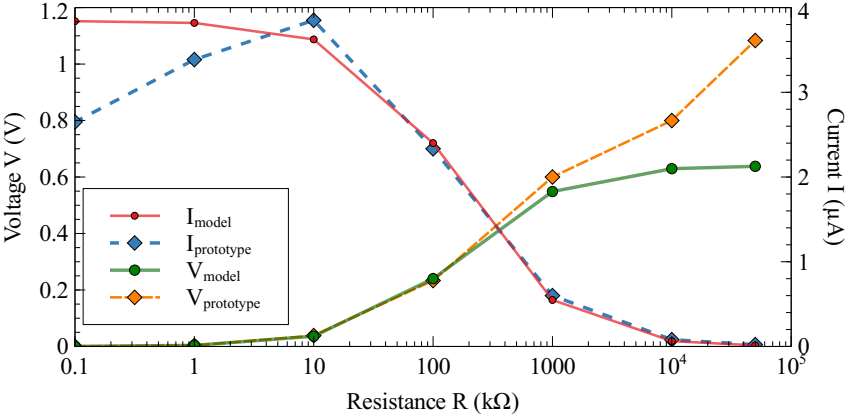


Figure 20. Piezoelectric harvesting system voltage and current

In the experiment, a combination of piezoelectric and thermoelectric harvesting systems was realized. To that end, the output wires of the two systems were connected in series to increase the amount of energy harvested. The total voltage is increased when two different sources are connected in series. The total voltage is the sum of the piezoelectric and thermoelectric voltages. Normally, the behavior of the thermoelectric generator depends on the gradient temperature, so when the resistance is low, the harvested power is higher. However, when the two systems are combined, the behavior of the harvested power is the combination of the behavior of the two systems. In this test case, it is observed that the behavior of the piezoelectric harvesting system is dominant. The shape of the harvested power starts at a low level when the resistance value is low. Then, it reaches a maximum value of around 100 kΩ. Beyond this point, the power curve is decreasing.

When the output power from the TEG and PEG harvesting systems is in the same range of value, the behavior of the PEG dominates the combined system due to impedance mismatching. Thus, an optimal resistance is determined to maximize the

output power. In the case when the output power from the TEG is in a greater range of value, the behavior of the combined system will tend to be linear according to the TEG behavior. Figure 21 shows the shape of the power curve under different values of load resistance.

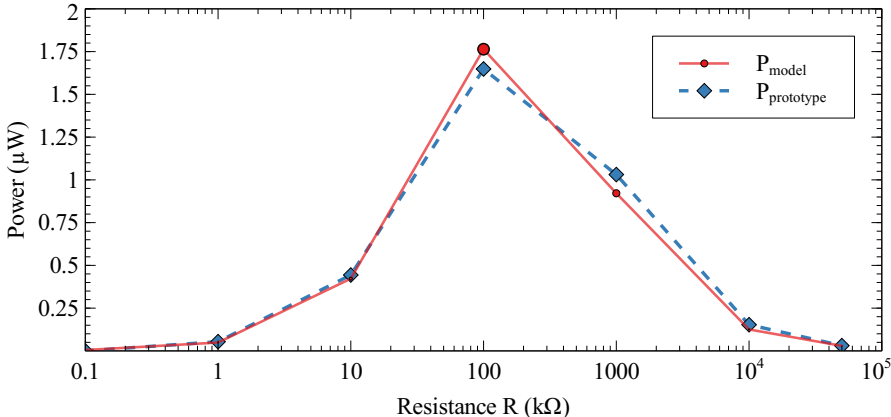


Figure 21. Piezo-thermoelectric harvesting system power

In figure 22, the voltage and the current are displayed under different resistance values.

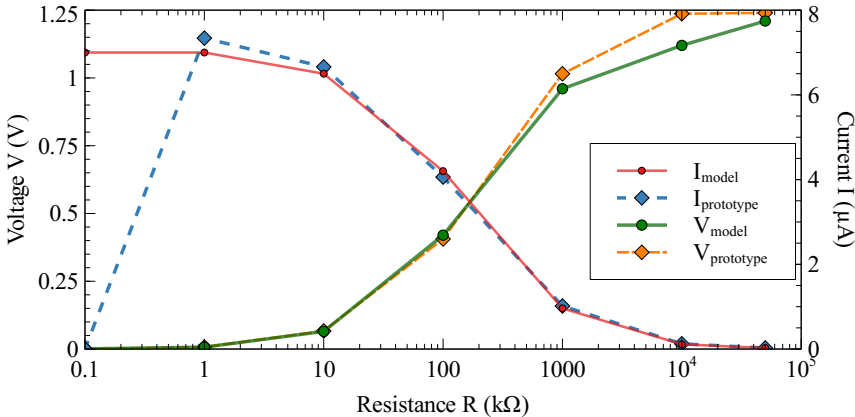


Figure 22. Piezo-thermoelectric harvesting system voltage and current

As for the piezoelectric harvesting system, the current is at its maximum value when the resistance is at its minimum, and it is decreasing when the resistance value is increasing. It can be noticed that an error of measurement exists on the value of the current of the prototype at 0.1 kΩ. However, in simulation, the highest value of the current at this resistance value can be retrieved. On the other hand, the voltage increases when the resistance value increases. Thus, the maximum value of the voltage is reached when the resistance is at its maximum when the circuit is nearly open.

4. Discussion and possible application

Because current road energy harvesting systems rely on a single source of energy—mechanical motions or thermal or temperature gradients caused by solar radiation—the energy sources are not constant and are intermittent. The intermittent nature of ambient energy sources is a significant impediment to the deployment of existing systems. The main benefit of the proposed solution is to address the intermittent issue by utilizing two energy sources: thermal and mechanical.

A comparative analysis of the proposed system compared to existing piezo-thermoelectric road harvesters showed Table 5. The main difference between this work and existing works is the methodology, which proposes electronic analogy modeling, electronic simulation, and low-cost prototype experimentation. However, the materials used in this work are not yet optimized to generate higher electrical output. The purpose of the low-cost prototype experimentation is first to validate the proposed electronic model.

Reference	Work specification	Methodology	Outputs
Mujaahid et al. [15]	Propose to exploit heat and vibration energy available on roadways and harvest energy without combination of the two harvesters.	- Experimental prototype of piezoelectric harvester - Experimental prototype of thermoelectric harvester - Laboratory experimentation	- Thermoelectric harvester : 1.55mW for 6 hours - Piezoelectric harvester : 9.83V for a stress of 235.04kPa
Pacis et al. [58]	Propose to exploit heat and vibration energy available on roadways and harvest energy with combination	- Experimentation in controlled environment - MATLAB simulation	Reported power : 2.75W to 4.33W
This work	Propose to exploit heat and vibration energy available on roadways and harvest energy with combination discussions of the two harvesters	- Electronic analogy modeling - Electronic simulation in SPICE environment - Low-cost experimental prototype of the combination	Low-cost prototype without material optimization : - Coupled piezo-thermoelectric harvester : 1.75μW

Table 5. Comparative analysis of the proposed piezo-thermoelectric harvester compared to existing piezo-thermoelectric harvesters applied on road

In real implementation, three scenarios were studied in this work about exploiting these two energy sources:

- With a hybrid combination: where the two energy sources are exploited to supply a common energy storage system even if they are not available in the same time;
- With a coupling combination: where the two energy sources are exploited simultaneously. It requires that they are available in the same time;
- Without a combination: where the two energy sources are exploited separately.

The energy harvester could be used for various applications on the roadway. The generated power per harvesting element ranges from μW to mW. However, when several elements are utilized along the roadway, the harvested energy becomes greater. A potential use of the harvester on the roadway is lighting, especially when the

infrastructure of the conventional electric grid cannot reach the roadway. Also, roadway monitoring systems could be supplied by harvested energy. If the harvesting system is widely deployed, it could produce sufficient energy to light houses along the roadway. Another advantage of a thermoelectric generator is the reduction of the urban heat effect.

4.1. With a hybrid combination

According to the results of the prototype in Paragraph 3.2, the piezo-thermoelectric harvesting system can be used as a hybrid energy source. A hybrid energy source is a combination of two or more energy sources to supply a common utilization (energy storage system). Most of the time, the energy sources used in a hybrid energy system are independent.

In the case of a road application, this hybrid combination appears to be a promising technique. Mostly because the two energy sources (thermal and mechanical) are independent and not necessarily available at the same moment. During the day, maybe the traffic is important and the weather is favorable to the thermoelectric system. However, during the night, even if the traffic is important, the weather could not be favorable to the thermoelectric system. In this case, the two energy sources could each independently supply the energy storage system. During the day, the traffic and the heat will charge the storage system, while during the night, only the traffic will charge the storage system.

It is recommended to use a supercapacitor as a storage system for this harvesting technology. The advantage of a supercapacitor compared to a battery is that the time for charging is shorter. For lighting or monitoring applications on road pavement, it is interesting that there are often passing vehicles to ensure rapid charging from piezoelectric harvesters. An additional advantage of the thermoelectric system is that it reduces the heat island effect if it is installed in a city.

4.2. With a coupling combination

The coupling combination consists of exploiting the two energy sources (thermal and mechanical) simultaneously. For road applications, as seen in Paragraph 4.1, the two energy sources are not necessarily available at the same moment. Then applying the coupling combination to the road pavements is not the best option.

This configuration is most suitable for the system when the thermal and mechanical vibration sources are available simultaneously. For instance, a coupling combination is interesting in harvesting the ambient energy of an electrical motor because there is thermal energy due to the electromagnetic and friction forces and mechanical vibration due to the rotation of the axis. Also, the thermoelectric harvesting system can contribute to evacuating the high temperature of the motor. Figure 21 shows that the coupling combination allows for the harvest of a higher amount of energy compared to only harvesting the piezoelectric (Figure 19). It is necessary to adjust the amount of energy

harvested through the output resistance from the two sources to harvest the maximum amount of energy.

The coupling combination can also be exploited in a high-temperature fluid circulation system. The thermoelectric harvesting system will collect the heat from the fluid pipe and transform it into electric energy. The piezoelectric harvesting system will exploit the mechanical vibration induced by the passage of the fluid in the pipe and transform it into electric energy. In this case, if the two energy sources are available at the same moment, then a coupling combination allows for the harvest of higher energy.

4.3. Without a combination

Another option is to not combine all of the two energy sources. This configuration may be useful in situations where there is only one source to exploit. In the case of road applications, it is interesting not to combine these two energy sources when one is unavailable, such as in a snowy country. In this situation, the thermoelectric harvesting system is inefficient because solar irradiation is not exploitable for the system. Then, mechanical vibration is the only available energy source, and a combination is not interesting.

Another scenario in which a roadway could be used is when there is no significant traffic on the road. It is the case with roads in southern countries with small populations when there are a limited number of passing vehicles. Due to the limited number of passing vehicles, installing a piezoelectric harvesting system may be uninteresting. However, the temperature of the road surface is high enough to warrant the installation of a thermoelectric harvesting system. People who live along the road will then have access to electricity, and the road's lifespan will be extended because it will not overheat.

The proposed harvesting system is designed for application on the road and aims to be reliable enough to generate energy for a long period of time. A reliability test is needed to verify the capability of the proposed configuration to deliver energy for a long period of time. Ju et al. [38] have conducted reliability tests on their piezoelectric harvesting device based on a Macro Fiber Composite cantilever. Their paper presented the results of a cyclic test to measure power degradation over 550,800 cycles of repeated operation, showing a power degradation trend ranging from 24.36% to 33.75% for different types of proof mass. Despite the power degradation, no deterioration of their Macro Fiber Composite cantilever has been observed, and improved long-term reliability has been confirmed by the use of a titanium alloy device. The proposed combined harvesting system exploits both piezoelectric and thermoelectric parts. Information concerning the lifetime of the piezoelectric transducer was not provided by the manufacturer. However, the thermoelectric generator used in this work assumes a lifetime expectancy of 200,000 hours. To verify the applicability of the proposed harvester on roadways, a structured approach for analyzing the reliability of the device should be carried out in future work. It involves considering safety events [88] like resistance against fatigue failure and the desired output electrical performance

of the device.

5. Conclusions

The modern way of life relies heavily on electrical power, but overuse has led to a decline in conventional energy sources. Environmental concerns have motivated researchers and governments to implement energy harvesting systems to address the intermittency issues of ambient energy sources. This paper proposes a new experimental combination prototype to address these issues. The prototype consists of a thermoelectric and piezoelectric harvesting system that exploits temperature gradients in road pavements and the mechanical vibration of passing vehicles to transform them into electricity.

The thermoelectric model consists of a DC voltage source in series with its internal resistance, while the piezoelectric model is a common resonating model of "mass+spring+damper+piezo" adapted to an electronic equivalent circuit. The combination model was established in a SPICE environment and simulated to understand the behavior of the combined system.

The final application depends on the existing configuration of the road. The TEG prototypes could generate up to 800 μW power, while the PEG prototypes could provide up to 0.6 μW separately. The advantage of the hybrid combination is that it exploits the maximum output power of the two energy sources and charges the storage system accordingly. The coupling combination provides up to 1.75 μW , higher than the isolated PEG but lower than the TEG.

This paper demonstrates a new possibility of exploiting and combining thermal and mechanical vibration energy in a road application, providing a starting reference in the field where most studies concern only one ambient energy source. The main innovative solution proposed in this work is the introduction of the possibility of combining piezoelectric and thermoelectric energy harvesting systems and the new design for a piezoelectric harvester with a vibration frequency.

Future works will focus on optimizing materials and power generation, comparing the energy cost for the combined piezo-thermoelectric energy harvester to other pavement standalone piezoelectric and thermoelectric energy harvesters, and developing an electronic optimization to maximize the combined harvested energy.

Data availability statement

The data that support the findings of this study are available upon request from the authors.

References

- [1] Harb A 2011 *Renewable Energy* **36** 2641–2654 ISSN 0960-1481 renewable Energy: Generation and Application URL <https://www.sciencedirect.com/science/article/pii/S0960148110002703>

- [2] Wei X, Liu X, Zheng C, Zhao H, Zhong Y, Amarasinghe Y and Wang P 2021 *Sustainable Energy Technologies and Assessments* **44** 101001 ISSN 2213-1388 URL <https://www.sciencedirect.com/science/article/pii/S2213138821000114>
- [3] Zhu J, Hu Z, Song C, Yi N, Yu Z, Liu Z, Liu S, Wang M, Dexheimer M G, Yang J and Cheng H 2021 *Materials Today Physics* **18** 100377 ISSN 2542-5293 URL <https://www.sciencedirect.com/science/article/pii/S2542529321000389>
- [4] Shakeel M, Rehman K, Ahmad S, Amin M, Iqbal N and Khan A 2021 *Renewable Energy* **167** 853–860 ISSN 0960-1481 URL <https://www.sciencedirect.com/science/article/pii/S0960148120319224>
- [5] Dhaundiyal A and Atsu D 2021 *Solar Energy* **218** 337–345 ISSN 0038-092X URL <https://www.sciencedirect.com/science/article/pii/S0038092X21001699>
- [6] Wang C, Song Z, Gao Z, Yu G and Wang S 2019 *Energy and Buildings* **183** 581–591 ISSN 0378-7788 URL <https://www.sciencedirect.com/science/article/pii/S0378778818324435>
- [7] Tahami S A, Gholikhani M, Nasouri R, Dessouky S and Papagiannakis A 2019 *Applied Energy* **238** 786–795 ISSN 0306-2619 URL <https://www.sciencedirect.com/science/article/pii/S0306261919301709>
- [8] Safa H 2020 *L'énergie Quelle transition énergétique?* (EDP Sciences) pp 13–26 URL <https://doi.org/10.1051/978-2-7598-0988-2-003>
- [9] Gholikhani M, Roshani H, Dessouky S and Papagiannakis A 2020 *Applied Energy* **261** 114388 ISSN 0306-2619 URL <https://www.sciencedirect.com/science/article/pii/S0306261919320756>
- [10] Ahmed A, Hassan I, Helal A S, Sencadas V, Radhi A, Jeong C K and El-Kady M F 2020 *iScience* **23** 101286 URL <https://pubmed.ncbi.nlm.nih.gov/32622264/>
- [11] Jeong C K, Hyeon D Y, Hwang G T, Lee G J, Lee M K, Park J J and Park K I 2019 *Journal of Materials Chemistry A* **7** 25481–25489 URL <https://pubs.rsc.org/en/content/articlelanding/2019/ta/c9ta09864j/unauth>
- [12] Jiang W, Yuan D, Xu S, Hu H, Xiao J, Sha A and Huang Y 2017 *Applied Energy* **205** 941 – 950 ISSN 0306-2619 URL <http://www.sciencedirect.com/science/article/pii/S0306261917311108>
- [13] Abdal-kadhim A M and Leong k S 2019 *International Journal of Integrated Engineering* **11** URL <https://publisher.uthm.edu.my/ojs/index.php/ijie/article/view/2348>
- [14] Ando Ny Aina R, Damien Ali Hamada F, Luc R and Wynand Jacobus Van Der Merwe S 2022 *International Journal of Pavement Research and Technology* 26 URL <https://link.springer.com/article/10.1007/s42947-022-00164-z>
- [15] Lallmamode M M and Al-Obaidi A M 2021 Harvesting energy from vehicle transportation on highways using piezoelectric and thermoelectric technologies *Journal of Physics: Conference Series* vol 2120 (IOP Publishing) p 012016 URL <https://iopscience.iop.org/article/10.1088/1742-6596/2120/1/012016/meta>
- [16] Khalili M, Biten A B, Vishwakarma G, Ahmed S and Papagiannakis A 2019 *Applied Energy* **253** 113585 ISSN 0306-2619 URL <https://www.sciencedirect.com/science/article/pii/S0306261919312590>
- [17] Xu T B, Siochi E J, Kang J H, Zuo L, Zhou W, Tang X and Jiang X 2013 *Smart Materials and Structures* **22** 065015 URL <https://iopscience.iop.org/article/10.1088/0964-1726/22/6/065015>
- [18] Guo L and Lu Q 2017 *Applied Energy* **208** 1071 – 1082 ISSN 0306-2619 URL <http://www.sciencedirect.com/science/article/pii/S0306261917313296>
- [19] Kim M, Hoegen M, Dugundji J and Wardle B L 2010 *Smart Materials and Structures* **19** 045023 URL <https://iopscience.iop.org/article/10.1088/0964-1726/19/4/045023/meta>
- [20] Cao Y, Li J, Sha A, Liu Z, Zhang F and Li X 2022 *Journal of Cleaner Production* **369** 133287 URL <https://www.sciencedirect.com/science/article/abs/pii/S0959652622028736>
- [21] Wang C, Zhou R, Wang S, Yuan H and Cao H 2023 *Energy* **270** 126896 URL <https://www.sciencedirect.com/science/article/abs/pii/S0360544223002906>

- [22] Wang S, Wang C, Yu G and Gao Z 2020 *Energy Conversion and Management* **207** 112571 ISSN 0196-8904 URL <http://www.sciencedirect.com/science/article/pii/S0196890420301084>
- [23] Ye J, Ding G, Wu X, Zhou M, Wang J, Chen Y and Yu Y 2023 *Materials Today Communications* **34** 105135 URL <https://www.sciencedirect.com/science/article/abs/pii/S2352492822019766>
- [24] Papagiannakis A, Dessouky S, Montoya A and Roshani H 2016 *Procedia Computer Science* **83** 758–765 ISSN 1877-0509 the 7th International Conference on Ambient Systems, Networks and Technologies (ANT 2016) / The 6th International Conference on Sustainable Energy Information Technology (SEIT-2016) / Affiliated Workshops URL <https://www.sciencedirect.com/science/article/pii/S1877050916301971>
- [25] Guo L and Lu Q 2019 *Applied Energy* **235** 963 – 977 ISSN 0306-2619 URL <http://www.sciencedirect.com/science/article/pii/S0306261918317446>
- [26] Zhou W, Penamalli G R and Zuo L 2011 *Smart Materials and Structures* **21** 015014 URL <https://iopscience.iop.org/article/10.1088/0964-1726/21/1/015014/pdf>
- [27] Khan F U and Qadir M U 2016 *Journal of Micromechanics and Microengineering* **26** 103001 ISSN 0960-1317, 1361-6439 URL <https://iopscience.iop.org/article/10.1088/0960-1317/26/10/103001>
- [28] Ouro-Koura H, Sotoudeh Z, Tichy J and Borca-Tasciuc D A 2022 *Energies* **15** 6105 ISSN 1996-1073 URL <https://www.mdpi.com/1996-1073/15/17/6105>
- [29] Li J, Ouro-Koura H, Arnou H, Nowbahari A, Galarza M, Obispo M, Tong X, Azadmehr M, Hella M M, Tichy J A *et al.* 2023 A novel comb design for enhanced power and bandwidth in electrostatic mems energy converters *2023 IEEE 36th International Conference on Micro Electro Mechanical Systems (MEMS) (IEEE)* pp 728–731 URL <https://ieeexplore.ieee.org/abstract/document/10052590/references#references>
- [30] Yen B C and Lang J H 2006 *IEEE Transactions on Circuits and Systems I: Regular Papers* **53** 288–295 URL <https://ieeexplore.ieee.org/abstract/document/1593935>
- [31] Li Z, Zuo L, Luhrs G, Lin L and Qin Y x 2012 *IEEE Transactions on vehicular technology* **62** 1065–1074 URL <https://ieeexplore.ieee.org/abstract/document/6399623>
- [32] Gholikhani M, Shirazi S Y B, Mabrouk G M and Dessouky S 2021 *Energy Conversion and Management* **230** 113804 URL <https://www.sciencedirect.com/science/article/abs/pii/S0196890420313273>
- [33] Zhang T, Kong L, Zhu Z, Wu X, Li H, Zhang Z and Yan J 2024 *Applied Energy* **353** 122047 URL <https://www.sciencedirect.com/science/article/abs/pii/S0306261923014113>
- [34] Lu X, Zhang H, Zhao X, Yang H, Zheng L, Wang W and Sun C 2021 *Nano Energy* **89** 106352 URL <https://www.sciencedirect.com/science/article/abs/pii/S2211285521006078>
- [35] Yang W, Chen J, Zhu G, Wen X, Bai P, Su Y, Lin Y and Wang Z 2013 *Nano Research* **6** 880–886 URL <https://link.springer.com/article/10.1007/s12274-013-0364-0>
- [36] Ibrahim A, Ramini A and Towfighian S 2018 *Journal of Sound and Vibration* **416** 111–124 URL <https://www.sciencedirect.com/science/article/abs/pii/S0022460X17308088>
- [37] Wei C and Jing X 2017 *Renewable and Sustainable Energy Reviews* **74** 1–18 URL <https://www.sciencedirect.com/science/article/abs/pii/S1364032117300837?via%3Dihub>
- [38] Ju S and Ji C H 2018 *Applied Energy* **214** 139–151 URL <https://www.sciencedirect.com/science/article/abs/pii/S0306261918300904>
- [39] Khan U and Kim S W 2016 *ACS nano* **10** 6429–6432 URL <https://pubs.acs.org/doi/abs/10.1021/acsnano.6b04213>
- [40] Tian J, Chen X and Wang Z L 2020 *Nanotechnology* **31** 242001 URL <https://iopscience.iop.org/article/10.1088/1361-6528/ab793e/meta>
- [41] Pascual-Muñoz P, Castro-Fresno D, Serrano-Bravo P and Alonso-Estébanez A 2013 *Applied Energy* **111** 324 – 332 ISSN 0306-2619 URL <http://www.sciencedirect.com/science/article/pii/S0306261913004029>
- [42] García A and Partl M N 2014 *Applied Energy* **119** 431 – 437 ISSN 0306-2619 URL <http://www.sciencedirect.com/science/article/pii/S0306261914000000>

- [//www.sciencedirect.com/science/article/pii/S0306261914000257](http://www.sciencedirect.com/science/article/pii/S0306261914000257)
- [43] Guldentops G, Nejad A M, Vuye C, den bergh W V and Rahbar N 2016 *Applied Energy* **163** 180 – 189 ISSN 0306-2619 URL <http://www.sciencedirect.com/science/article/pii/S0306261915014518>
- [44] Mallick R B, Chen B L and Bhowmick S 2012 *International Journal of Sustainable Engineering* **5** 159–169 ISSN 1939-7038 URL <https://www.tandfonline.com/doi/citedby/10.1080/19397038.2011.574742>
- [45] Wu S, Chen M, Wang H and Zhang Y 2009 *International Journal of Pavement* URL [http://www.ijprt.org.tw/mailweb/files/sample/V2N4\(2\).pdf](http://www.ijprt.org.tw/mailweb/files/sample/V2N4(2).pdf)
- [46] Hasebe M, Kamikawa Y and Meiarashi S 2006 Thermoelectric generators using solar thermal energy in heated road pavement *2006 25th international conference on thermoelectrics* (IEEE) pp 697–700 URL <https://ieeexplore.ieee.org/abstract/document/4133389/>
- [47] Guo L and Lu Q 2017 *Renewable and Sustainable Energy Reviews* **72** 761–773 ISSN 1364-0321 URL <https://www.sciencedirect.com/science/article/pii/S136403211730103X>
- [48] Datta U, Dessouky S and Papagiannakis A 2017 *Transportation Research Record* **2628** 12–22 URL <https://doi.org/10.3141/2628-02>
- [49] Wei J, Hui J, Wang T, Wang Y, Guo Y, Zhang S, Zhang Y and Qiao X 2023 *Sustainable Energy & Fuels* **7** 248–262 URL <https://pubs.rsc.org/en/content/articlehtml/2022/se/d2se01572b>
- [50] Twaha S, Zhu J, Yan Y and Li B 2016 *Renewable and Sustainable Energy Reviews* **65** 698 – 726 ISSN 1364-0321 URL <http://www.sciencedirect.com/science/article/pii/S1364032116303653>
- [51] Wu G and Yu X B 2013 *International Journal of Pavement Research and Technology* **6** 73 URL <https://pdfs.semanticscholar.org/9a74/d488bc881a9f8935c312e7f8478a1e437011.pdf>
- [52] Yoon K S, Hong S W and Cho G H 2017 *IEEE Journal of Solid-State Circuits* **53** 1049–1060 URL <https://ieeexplore.ieee.org/document/8232464>
- [53] Li Y, Liu Y, Liu X, Wang X and Li Q 2019 *IEICE Electronics Express* 16–20190066 URL https://www.jstage.jst.go.jp/article/elex/16/6/16_16.20190066/_article/-char/ja
- [54] Dessai S and Dessai A 2016 Design of piezoelectric-thermoelectric hybrid energy harvester for wireless sensor network *Proc. Int. Conf. Smart Electron.(ICSES)* pp 78–81 URL <http://i3cpublications.org/vol3-issue3/IJTS03031916ICSES16.pdf>
- [55] Oh Y, Kwon D S, Eun Y, Kim W, Kim M O, Ko H J, Kang S G and Kim J 2019 *Int. J. of Precis. Eng. and Manuf.-Green Tech.* **6** 691–698 ISSN 2198-0810 URL <https://doi.org/10.1007/s40684-019-00132-2>
- [56] Chen Z, Xia Y, Shi G, Xia H, Wang X, Qian L and Ye Y 2021 *Journal of Intelligent Material Systems and Structures* **32** 2260–2272 URL <https://journals.sagepub.com/doi/abs/10.1177/1045389X21991238>
- [57] Jella V, Ippili S, Eom J H, Kim Y J, Kim H J and Yoon S G 2018 *Nano Energy* **52** 11 – 21 ISSN 2211-2855 URL <http://www.sciencedirect.com/science/article/pii/S2211285518305123>
- [58] Pacis M, Magwili G, Cabrera J, Princillo K and Soriaga R 2022 Integrated piezoelectric and thermoelectric generator harvesting device for asphalt road surfaces *2022 IEEE 14th International Conference on Humanoid, Nanotechnology, Information Technology, Communication and Control, Environment, and Management (HNICEM)* (IEEE) pp 1–6 URL <https://ieeexplore.ieee.org/abstract/document/10109360>
- [59] Ahmad S, Abdul Mujeebu M and Farooqi M A 2019 Energy harvesting from pavements and roadways: A comprehensive review of technologies, materials, and challenges URL <https://onlinelibrary.wiley.com/doi/full/10.1002/er.4350https://onlinelibrary.wiley.com/doi/abs/10.1002/er.4350https://onlinelibrary.wiley.com/doi/10.1002/er.4350>
- [60] Safari A and Akdoğan E K 2008 *Piezoelectric and acoustic materials for transducer applications* (Springer) ISBN 9780387765389 URL <https://link.springer.com/book/10.1007/978-0-387-76540-2>

- [61] Beeby S P, Tudor M J and White N M 2006 *Measurement Science and Technology* **17** R175–R195 URL <https://iopscience.iop.org/article/10.1088/0957-0233/17/12/R01/meta>
- [62] Copper A 2010 *A Guide to Working With Copper and Copper Alloys* (www.copper.org/) URL https://www.copper.org/publications/pub_list/pdf/a1360.pdf
- [63] Jiang W, Yuan D, Xu S, Hu H, Xiao J, Sha A and Huang Y 2017 *Applied Energy* **205** 941–950 URL <https://www.sciencedirect.com/science/article/pii/S0306261917311108?via%3Dihub>
- [64] Gnip I, Vėjelis S and Vaitkus S 2012 *Energy and Buildings* **52** 107–111 URL <https://doi.org/10.1016/j.matdes.2014.12.024>
- [65] 2011 Phase change materials - an overview URL <https://www.sciencedirect.com/topics/materials-science/phase-change-materials>
- [66] Song Y, Yang C H, Hong S K, Hwang S J, Kim J H, Choi J Y, Ryu S K and Sung T H 2016 *International Journal of Hydrogen Energy* **41** 12563–12568 ISSN 03603199 URL <http://dx.doi.org/10.1016/j.ijhydene.2016.04.149>
- [67] Upadhye V and Agashe S **49** 286–292 ISSN 0020-2940 publisher: SAGE Publications Ltd URL <https://doi.org/10.1177/00202940166663974>
- [68] Haider M F, Giurgiutiu V, Lin B and Yu L **26** 095019 ISSN 0964-1726 publisher: IOP Publishing URL <https://dx.doi.org/10.1088/1361-665X/aa785f>
- [69] Thermoelectrics handbook: Macro to nano URL <https://doi.org/10.1201/9781420038903>
- [70] Karri N K and Mo C **47** 6101–6120 ISSN 1543-186X URL <https://doi.org/10.1007/s11664-018-6505-1>
- [71] Meng F, Chen L and Sun F 2012 *International Journal of Energy and Environment* **3** 137–150 URL http://ijee.ieefoundation.org/vol3/issue1/IJEE_14_v3n1.pdf
- [72] Horak E, De Beer M, Van Zyl G, Maina J and Fakra D A H 2022 *CivilEng* 12 URL <https://www.mdpi.com/2673-4109/3/2/27>
- [73] HebeiIT Datasheet - tec1-12706 peltier module URL <https://peltiermodules.com/peltier-datasheet/TEC1-12706.pdf>
- [74] KINGSTATE Datasheet - piezoelectric transducer kpsgl100 URL <https://www.gmelectronic.com/data/attachments/dsh.641-017.1.pdf>
- [75] MacDonald D K C and Tuomi D 1963 *Journal of The Electrochemical Society* **110** 206C URL <https://doi.org/10.1149/1.2425888>
- [76] Siouane S, Jovanović S and Poure P 2017 *Energies* **10** ISSN 1996-1073 URL <https://www.mdpi.com/1996-1073/10/3/386>
- [77] Tahami A, Gholiakhani M, Dessouky S, Montoya A, Papagiannakis A T, Fuentes L and Walubita L F 2021 *International Journal of Sustainable Engineering* **00** 1–17 ISSN 1939-7038 URL <https://doi.org/10.1080/19397038.2021.1924892>
- [78] Zhu X, Yu Y and Li F 2019 *Construction and Building Materials* **228** 116818 ISSN 0950-0618 URL <https://www.sciencedirect.com/science/article/pii/S0950061819322482>
- [79] Abdelkefi A, Najjar F, Nayfeh A H and Ayed S B 2011 *Smart Materials and Structures* **20** 115007 URL <https://iopscience.iop.org/article/10.1088/0964-1726/20/11/115007/meta>
- [80] Fan K, Chang J, Chao F and Pedrycz W 2015 *Energy Conversion and Management* **96** 430–439 URL <https://www.sciencedirect.com/science/article/pii/S0196890415002241>
- [81] Rendon-Hernandez A A, Ferrari M, Basrouf S and Ferrari V 2019 *Journal of Physics: Conference Series* **1407** 012058 URL <https://doi.org/10.1088/1742-6596/1407/1/012058>
- [82] Guyomar D, Badel A, Lefeuvre E and Richard C 2005 *IEEE Transactions on Ultrasonics, Ferroelectrics and Frequency Control* **52** 584–595 URL <https://ieeexplore.ieee.org/abstract/document/1428041>
- [83] Minazara E, Vasic D, Costa F and Poulin G 2006 *Ultrasonics* **44** e699–e703 ISSN 0041-624X proceedings of Ultrasonics International (UI'05) and World Congress on Ultrasonics (WCU) URL <https://www.sciencedirect.com/science/article/pii/S0041624X06001661>
- [84] Vasic D and Costa F 2011 *Applications des éléments piézo-électriques en électronique de puissance* D3235 (Techniques de l'Ingénieur) URL <https://hal.archives-ouvertes.fr/hal-00811666>

- [85] Goudarzi M, Niazi K and Besharati M K URL https://www.ipme.ru/e-journals/MPM/no_11613/MPM116_04_niazi.pdf
- [86] Zhou Y, Zhang S, Xu X, Liu W, Zhang S, Li G and He J 2020 *Nano Energy* **69** 104397 ISSN 2211-2855 URL <http://www.sciencedirect.com/science/article/pii/S2211285519311115>
- [87] Shu Y C and Lien I C 2006-12-01 *Smart Materials and Structures* **15** 1499–1512 ISSN 0964-1726, 1361-665X URL <https://iopscience.iop.org/article/10.1088/0964-1726/15/6/001>
- [88] Yoon H and Youn B D 2018 *Smart Materials and Structures* **28** 025010 URL <https://iopscience.iop.org/article/10.1088/1361-665X/aaf116/meta>